AD-A041 945 CALIFORNIA UNIV BERKELEY HYDRAULIC ENGINEERING LAB F/G 8/3
SEDIMENT SUSPENSION AND TURBULENCE IN AN OSCILLATING FLUME.(U)
APR 77 T C MACDONALD DACW72-71-C-0024
UNCLASSIFIED HEL-2-39-SUPPL CERC-TP-77-4 NL

1 OF 1
ADA041945

END

DATE FILMED
8-77

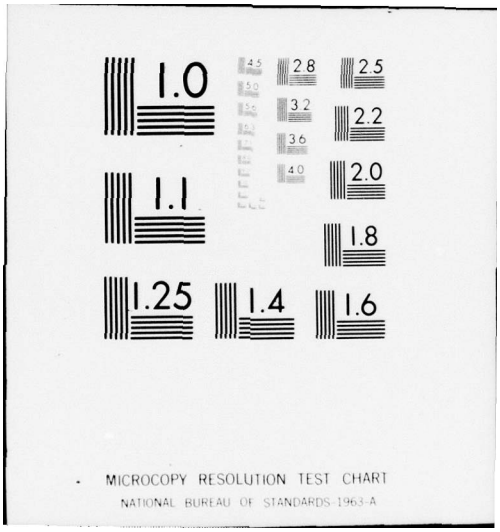
1.0
1.1
1.25
1.4
1.6
1.8
2.0
2.2
2.5
2.8
3.2
3.6
4.0
4.5
5.0
MICROCOPY RESOLUTION TEST CHART
NATIONAL BUREAU OF STANDARDS-1963-A

12

TP 77-4

Sediment Suspension and Turbulence in an Oscillating Flume

by
Thomas C. MacDonald

TECHNICAL PAPER NO. 77-4
APRIL 1977

Approved for public release;
distribution unlimited.

Prepared for
U.S. ARMY, CORPS OF ENGINEERS
COASTAL ENGINEERING
RESEARCH CENTER
Kingman Building
Fort Belvoir, Va. 22060

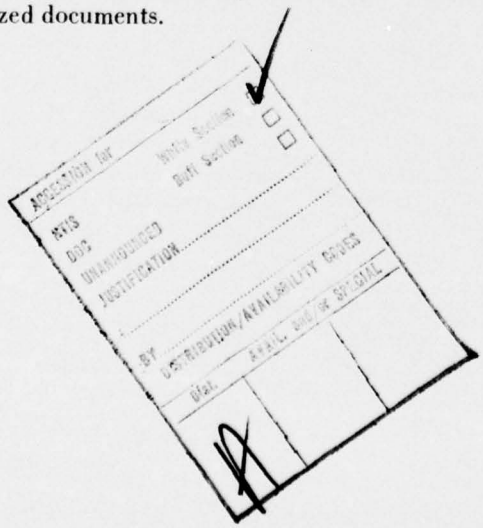

(18) CERC

UNCLASSIFIED

SECURITY CLASSIFICATION OF THIS PAGE (When Data Entered)

REPORT DOCUMENTATION PAGE	READ INSTRUCTIONS BEFORE COMPLETING FORM
1. REPORT NUMBER (19) TP-77-4	2. GOVT ACCESSION NO.
3. RECIPIENT'S CATALOG NUMBER	
4. TITLE (and Subtitle) (6) SEDIMENT SUSPENSION AND TURBULENCE IN AN OSCILLATING FLUME	5. TYPE OF REPORT & PERIOD COVERED (9) Technical Paper
6. PERFORMING ORG. REPORT NUMBER (14) HEL-2-39-Supp1	
7. AUTHOR(s) (10) Thomas C. MacDonald	8. CONTRACT OR GRANT NUMBER(s) (15) DACW72-71-C-0024
9. PERFORMING ORGANIZATION NAME AND ADDRESS University of California Hydraulic Engineering Laboratory Berkeley, California 94720	10. PROGRAM ELEMENT, PROJECT, TASK AREA & WORK UNIT NUMBERS D31193
11. CONTROLLING OFFICE NAME AND ADDRESS Department of the Army Coastal Engineering Research Center (CERRE-CP) Kingman Building, Fort Belvoir, Virginia 22060	12. REPORT DATE (11) April 1977 13. NUMBER OF PAGES (12) 83p. 80
14. MONITORING AGENCY NAME & ADDRESS (if different from Controlling Office)	15. SECURITY CLASS. (of this report) UNCLASSIFIED 15a. DECLASSIFICATION/DOWNGRADING SCHEDULE

16. DISTRIBUTION STATEMENT (of this Report)

Approved for public release; distribution unlimited.

17. DISTRIBUTION STATEMENT (of the abstract entered in Block 20, if different from Report)

18. SUPPLEMENTARY NOTES

19. KEY WORDS (Continue on reverse side if necessary and identify by block number)

Oscillating flume Sediment suspension Turbulence Waves

20. ABSTRACT (Continue on reverse side if necessary and identify by block number)

An experimental study measured suspended-sediment concentrations and turbulence above the bottom of a specially designed oscillating flume. A total of 73 concentration distributions was measured for a single fixed-bottom roughness and the same specific gravity (1.25) of sediment. Three different sediment sizes were used, 65 experiments with the same size. These experiments show a simple exponential distribution, except near the bottom, as previously found by other investigators. The slope of the concentration

(Continued) → next page

DD FORM 1 JAN 73 1473 EDITION OF 1 NOV 65 IS OBSOLETE

UNCLASSIFIED

SECURITY CLASSIFICATION OF THIS PAGE (When Data Entered)

cont

distribution is in the range of -5 to -15 per foot (-16 to -50 per meter) for the experiments. For the limited data on other sizes, the slope of the concentration distribution becomes more negative as fall velocity increases.

Turbulent velocity fluctuations measured with a hot-film anemometer are normally distributed with mean zero for measurements at two elevations above the bed, well outside the viscous boundary layer. The root mean square of the velocity fluctuations decreases exponentially with distance above the bed, and at the bed, increases approximately linearly with increase in flume velocity.

When extrapolated to typical field conditions seaward of the breaker, these experiments demonstrate the importance of fall velocity, maximum wave-induced bottom velocity, and turbulent velocity fluctuations in controlling sediment suspension by shoaling waves. However, comparisons of data obtained with the lightweight sediment in these experiments and the probable motion of quartz sand in the field suggest that sediment suspensions caused by shoaling waves offshore of the breaker are likely to be limited.

PREFACE

This report is published to provide coastal engineers with an analysis of data on suspensions of sediment produced by oscillatory motion in a specialized laboratory facility at the Hydraulic Engineering Laboratory (HEL), University of California, Berkeley. The work was carried out under the coastal processes program of the U.S. Army Coastal Engineering Research Center (CERC).

The report was prepared by Dr. Thomas C. MacDonald, a former graduate student at the Hydraulic Engineering Laboratory, and now an engineer with Leeds, Hill, and Jewett, San Francisco, under CERC Contract No. DACW72-71-C-0024. The report is a modification of report No. HEL 2-39 which was originally issued by the Hydraulic Engineering Laboratory.

The author acknowledges with sincere gratitude the active supervision and counsel of the late Professor H.A. Einstein, the advice and the opportunity to participate in this project provided by Professor J.W. Johnson, and the assistance of Professors J. Harder and L. Talbot during the experiments and in the preparation of the report. The cooperation and assistance of the staff of the Hydraulic Engineering Laboratory are gratefully acknowledged, especially W.A. Hewett, J.C. Allison, and R.W. Cambell.

Dr. M.M. Das, former Hydraulic Engineer in the Coastal Processes Branch, and Dr. C.J. Galvin, Jr., Chief, Coastal Processes Branch, were the CERC contract monitors, under the general supervision of R.P. Savage, Chief, Research Division.

Comments on this publication are invited.

Approved for publication in accordance with Public Law 166, 79th Congress, approved 31 July 1945, as supplemented by Public Law 172, 88th Congress, approved 7 November 1963.

JOHN H. COUSINS
Colonel, Corps of Engineers
Commander and Director

CONTENTS

TABLES

CONTENTS--Continued

FIGURES

CONTENTS

FIGURES--Continued

CONVERSION FACTORS, U.S. CUSTOMARY TO METRIC (SI)
UNITS OF MEASUREMENT

U.S. customary units of measurement used in this report can be converted to metric (SI) units as follows:

Multiply	by	To obtain
inches	25.4	millimeters
	2.54	centimeters
square inches	6.452	square centimeters
cubic inches	16.39	cubic centimeters
feet	30.39	centimeters
	0.3048	meters
square feet	0.0929	square meters
cubic feet	0.0283	cubic meters
yards	0.9144	meters
square yards	0.836	square meters
cubic yards	0.7646	cubic meters
miles	1.6093	kilometers
square miles	259.0	hectares
knots	1.8532	kilometers per hour
acres	0.4047	hectares
foot-pounds	1.3558	newton meters
millibars	1.0197×10^{-3}	kilograms per square centimeter
ounces	28.35	grams
pounds	453.6	grams
	0.4536	kilograms
ton, long	1.0160	metric tons
ton, short	0.9072	metric tons
degrees (angle)	0.1745	radians
Fahrenheit degrees	5/9	Celsius degrees or Kelvins[1]

[1]To obtain Celsius (C) temperature readings from Farenheit (F) readings, use formula: $C = (5/9)(F - 32)$.

To obtain Kelvin (K) readings, use formula: $K = (5/9)(F - 32) + 273.15$.

SYMBOLS AND DEFINITIONS

A	exponential decay rate of the velocity scale
C	sediment concentration
C_n	calibration nozzle coefficient
C_o	sediment concentration at the base elevation
D	representative roughness diameter
d	water depth
E	sediment exchange coefficient
E'	output voltage of hot-film bridge
E_o	output voltage of hot-film bridge with sensor in still water
g	acceleration due to gravity
H	crest-to-trough wave height
I	output voltage of photoelectric cell
I'	output voltage of photoelectric cell for ambient light
I_o	output voltage of photoelectric cell with light beam passing through clear water
K'	constant of proportionality between directional components of turbulent velocity fluctuations
k	wave number
L	amplitude of flume oscillation
l	length of surface wave
l_e	length scale for oscillating and unidirectional flow
M	exponential decay rate of sediment concentration of oscillating flow
n	Manning's roughness coefficient
R	hydraulic radius
r	horizontal oscillating velocity

SYMBOLS AND DEFINITIONS--Continued

S	slope of the energy gradeline
s	velocity scale for oscillating flow
s_o	velocity scale at base elevation for oscillating flow
T	period of flume oscillation
t	time
U_e	effective heat transfer velocity for anemometer sensor
U_o	oscillating flow velocity
u	horizontal flow velocity
u'	longitudinal component of turbulent velocity fluctuations
u_*	shear velocity
V	peak velocity of oscillating sensor
V_e	effective heat transfer velocity
V_{mean}	mean velocity across calibration jet
$V_{meas.}$	centerline velocity of calibration jet as determined from voltage measurements
V_s	sediment-settling velocity
v	velocity scale for unidirectional flow theory
v'	vertical component of turbulent velocity fluctuations
w	angular frequency
X	horizontal displacement of fluid particle in oscillating flow
x	horizontal distance, positive in direction of wave travel
Y	elevation above base elevation
y	vertical distance, positive up from mean water surface
Z	theoretical exponent of unidirectional flow concentration distribution

SYMBOLS AND DEFINITIONS--Continued

Z'	measured exponent of unidirectional flow concentration distribution
Δ	vertical displacement of fluid particle in oscillating flow
δ	thickness of the boundary layer
ρ	water density
τ	shear stress at elevation Y in unidirectional flow
τ_o	shear stress at bed in unidirectional flow
θ	phase angle

SEDIMENT SUSPENSION AND TURBULENCE IN AN OSCILLATING FLUME

by
Thomas C. MacDonald

I. INTRODUCTION

Sediment transport by waves approaching the shore has been analyzed in two ways. Inshore of the breaker zone, the extremely complex flow patterns and turbulence resulting from the breaking waves have necessitated only a qualitative approach to sediment transport with quantitative estimates based on field measurements. Offshore of the breaker zone in relatively deep water, the problem of sediment transport can be approached in a more theoretical manner. In this zone, sediment transport studies are simplified because there is no turbulence in the flow field from breaking waves and the flow condition near the ocean bottom can be better estimated from linear wave theory. This report concerns sediment transport offshore of the breaker zone.

Laboratory and field observations indicate that, as in unidirectional flow, sediment transport at the ocean bottom offshore of the breaker zone is of two different types--bedload and suspended load. The distinguishing feature between these two types of transport is that in suspended transport the entire weight of the sediment is continuously supported by the fluid; whereas, in bedload transport the sediment rolls, skips, and jumps along the bed and therefore its weight is partially supported by the stationary bed. For moving sediment to be supported by the bed means that the regime of bedload transport is contained in a thin layer adjacent to the stationary bed, two-grain diameters thick as proposed by Einstein (1950). The majority of the sediment in motion in this area is bedload and thus most research has concentrated on the turbulent boundary layer and the oscillatory bedload rate due to wave action (Li, 1954; Manohar, 1955; Kalkanis, 1957, 1964; Abou-Seida, 1965). Sufficient advances in the theory of bedload movement in an oscillating flow have warranted studying the suspended load to determine: (a) Approximately, what percentage of offshore movement is due to suspended load, i.e., a second-order approximation to total transport; and (b) if any of the now-predicted bedload is partially suspended load.

This investigation develops, from an empirical approach, a method for predicting the distribution of suspended-sediment concentration based on the hydraulic flow conditions; i.e., surface wave amplitude and period, depth, sediment characteristics, and bottom roughness conditions. Although only one bottom roughness was studied, the resulting method is general enough to be extended to other roughness conditions by additional experimentation. The suspended distributions, when used in conjunction with the bedload function of Kalkanis (1964), should give a better approximation of the total sediment transport.

As in Kalkanis' bedload function, the approach to the suspended load is based on many of the same principles proposed by Einstein (1950) in his theory of bedload and suspended-load transport in unidirectional flow. Analysis of suspended load in oscillating flow is more complicated than that of unidirectional flow because of two factors. First, in unidirectional open channel flow the entire depth of flow is turbulent and the relatively high turbulent velocity fluctuations allow the sediment exchange coefficient to be approximated by the momentum exchange coefficient which can be obtained from the shear-stress distribution. In oscillatory flow this is not possible. Both laboratory and field observations indicate that suspension of sediment occurs to depths considerably above the boundary layer in an area where the shear stresses due to the oscillating motion are extremely small and difficult to measure. Although it may be possible to express a sediment exchange coefficient in the boundary layer as a function of the mean shear stress, this would not provide a means of estimating the sediment exchange coefficient above the boundary layer. Therefore, a sediment exchange coefficient which is not based on a shear-stress distribution must be found.

The second factor concerns the magnitude of the turbulent velocity fluctuations. Offshore of the breaker zone where the flow velocities near the bed are low, only a small part of the wave energy is dissipated by friction at the boundary. The remaining wave energy is lost inshore by the breaking waves. Because of the relatively low intensity of turbulence in this offshore area, the vertical velocity fluctuations are of the same order of magnitude as the settling velocity of the sediment. Under these conditions, the sediment exchange coefficient is highly dependent on the sediment-settling velocity. Therefore, measured distributions of turbulent velocity fluctuations and sediment concentrations must be used in analyzing the upward turbulent flux and downward turbulent and gravitational flux for each sediment-settling velocity.

To obtain a relationship between sediment suspension and flow hydraulics in an oscillating flow, concentration distributions for various flow conditions must be measured. The sediment exchange coefficient is determined from these measurements. Next, the turbulent velocity fluctuation distribution with time at a constant elevation and its distribution with elevation must be measured. This measurement will yield the information necessary to describe the fluid exchange. The distribution with elevation will yield a velocity scale, one of the two variables composing the sediment exchange coefficient. From the sediment exchange coefficient and the velocity scale, the second variable (the length scale or its associated time scale) can be calculated. Knowledge of these fundamental variables of suspension as a function of the flow hydraulics should lead to a practical method of estimating the suspended-load distribution, and indicate the important variables of suspension in an oscillating flow.

The only other requirement for a solution to the suspended load is a knowledge of a base concentration as a function of flow hydraulics. The base concentration is determined from Kalkanis' (1964) bedload theory, being the concentration at the top of the bedload layer.

Combination of the bedload and suspended load will predict the total amount of sediment in motion under specified wave and boundary conditions. By superimposing a constant unidirectional flow, such as the mass transport or a coastal current, the amount of sediment transport can be estimated.

In this investigation, as in many research projects, the experimental research preceded the development of a suitable method of describing sediment suspension. For this reason a description of the experiments and their results will be given first, followed by a discussion of how the results can be used to predict the sediment suspension load.

II. CONCENTRATION DISTRIBUTIONS

1. Experimental Apparatus.

Experiments and observations indicate that near the ocean bottom offshore of the breaker zone in relatively deep water, sediment is held in suspension. This is due to the turbulence resulting from the dissipation of wave energy on the rough ocean bed. For waves with a small surface slope, where $\partial/\partial x \ll \partial/\partial y$, the fluid motion can be approximated from linear wave theory. The equations describing the horizontal and vertical displacement of a fluid particle are given by the expressions from Lamb (1932):

$$X = \left(\frac{1}{2}H\right) \{\cosh[k(y+d)]/\sinh(k\ d)\} \cos(k\ x - w\ t) \qquad (1)$$

$$\Delta = \left(\frac{1}{2}H\right) \{\sinh[k(y+d)]/\sinh(k\ d)\} \sin(k\ x - w\ t) \qquad (2)$$

where

d = the water depth

y = the distance from the mean water surface measured negatively downward

H = the crest-to-trough wave height

$k = 2\pi/1$

1 = the length of the surface wave

$w = 2\pi/T$

T = the period of the surface wave

The corresponding velocity components are obtained by differentiation with respect to time of the above equations to give:

$$u = \left(\frac{1}{2}H\right) w \{\cosh[k(y+d)]/\sinh(k\ d)\} \sin(k\ x - w\ t) \qquad (3)$$

$$r = \left(-\frac{1}{2}H\right) w \{\sinh[k(y+d)]/\sinh(k\ d)\} \cos(k\ x - w\ t) \qquad (4)$$

From these equations it is evident that the vertical component of the displacement and velocity becomes smaller as the distance from the surface increases. At the bottom, where y = -d, the motion degenerates into a simple harmonic oscillation in the x-direction. It is this horizontal harmonic oscillation which is of first-order importance in producing turbulence and suspension of sediment. The equations also indicate that the magnitudes of the horizontal displacement and velocity change slightly with depth near the ocean bottom and can therefore be considered constant in the region of sediment suspension. For example, consider a 5-foot-high wave with a wavelength of 150 feet and a period of 10 seconds in a water depth of 50 feet. Equation (3) indicates the horizontal velocity at y = -d is u = 0.393 sin(kx-wt) feet per second and that for y = -d + 5 (5 feet above the bed), the horizontal velocity is u = 0.401 sin(kx-wt). The sediment suspension measurements which will be discussed later indicate that the regime of measurable sediment concentrations is well within the bottom 5 feet of water depth for this typical wave condition. (Measurable sediment concentrations were actually found within 1 foot of the bed.) The change in horizontal velocity in the bottom 5 feet of water depth is only 2 percent. Therefore, to design an experimental apparatus to simulate the flow conditions near the ocean floor, the horizontal flow velocity above the boundary layer can be considered constant and equal to the value given by equation (3) for y = -d. Equation (4) indicates that for the wave condition discussed above the vertical flow velocity at y = -d is zero, and at an elevation of 5 feet above the bed is 0.082 cos (kx-wt). The fact that the vertical velocity only increases slightly in the 5 feet above the bed and that its motion is symmetrical suggests that the vertical velocity has no effect on the suspension of sediment.

With the above assumptions of a constant horizontal oscillating velocity and zero vertical oscillating velocity above the boundary layer, the turbulent flow conditions which exist near the ocean floor are easily approximated. By superimposing a constant velocity equal to that given by equation (3) for y = -d but opposite in sign, there would be no motion in the fluid above the boundary layer, the distribution of velocities in the boundary layer would be inverted, and the bed would be oscillating at the simple harmonic given by equation (3) for y = -d.

It is now only necessary that the physical apparatus which duplicates these flow conditions contains a water depth greater than the thickness of the boundary layer. Kalkanis (1957) made velocity distribution measurements in a flume containing a still body of water with an oscillating

rough bed. Kalkanis (1964) showed that the velocity distribution in an oscillating flow with the same assumptions as described above can be approximated by:

$$u/u_o = [1 + f_1^2(Y) - 2f_1(Y) \cos f_2(Y)]^{1/2} \sin(wt + \theta) \qquad (5)$$

where

$$f_1(Y) = \exp(Y \cdot 10^3/a\beta D), \qquad (6)$$

$$f_2(Y) = 0.5(\beta Y)^{0.67}, \qquad (7)$$

and $\sin(wt + \theta)$ describes the variance of the velocity with time and phase angle. In equations (6) and (7), Y is the elevation above the bed measured positively upwards; a is the amplitude of bed oscillation; $\beta = (w/2\nu)^{1/2}$; ν is the kinematic viscosity; and D is the representative roughness diameter. For the flume roughness conditions used in this investigation ($D = 0.05$ foot), and the flow velocities studied (0.67 foot $< a <$ 2.0 feet and 2.0 seconds $< T <$ 15.0 seconds), equation (5) indicates the boundary layer thickness is no more than a few millimeters thick.

To approximate the shear stresses and therefore the turbulence conditions near the ocean bed for a given water depth, wave period, and amplitude, a flume having a moving bed under a still body of water was used. The frame of reference, which describes the prototype fluid motion under the above assumed conditions, is then moving with the bed. It is only necessary to oscillate the bed in the harmonic motion described by the linear wave theory for $y = -d$. The swing flume used in this investigation duplicates, on a one-to-one scale, these conditions.

The swing flume is shown in Figure 1(a). The flume bed is shaped to an arc segment of a circle with an 8.92-foot radius, a 13.33-foot chord length, and a 12-inch width. The flume, suspended from the ceiling of the laboratory, is free to rotate about its center of curvature. The flume is oscillated about its center position by a 1.5-horsepower variable-speed motor connected to a drive wheel with an eccentric arm. The eccentric arm is connected by a 10-foot connecting rod to a linkage fixed to the flume bottom. The linkage at the flume is adjustable to allow correction of the asymmetry of motion which would result from a change in eccentricity. Variations in eccentricity and motor speed allow the amplitude and frequency of oscillation to be varied over a wide range of prototype wave conditions.

Within the flume is a stationary horizontal board, slightly less than 12 inches wide, 8 feet long, and at an elevation of 12 inches above the lowest point of the curved bottom. The board, which is separately supported from the ceiling of the building and is not connected to the flume, suppresses any standing surface waves in the flume caused by the flume motion. The fluid at this elevation must remain stationary to conform to the flow conditions described above.

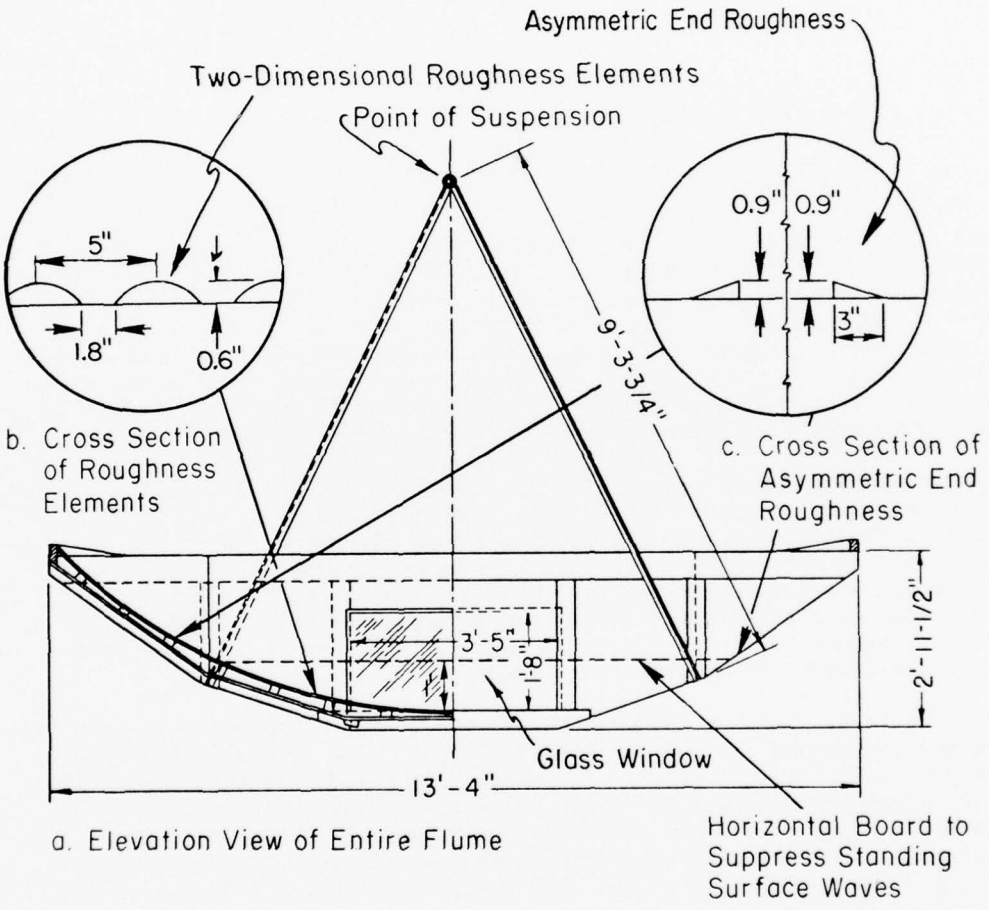

Figure 1. Swing flume.

The shape of the artificial bed roughness (Fig. 1,b) was determined by experiments. A large quantity of the artificial plastic sediment used in concentration measurements was put into the smooth-bottomed flume. The flume was oscillated at various amplitudes and periods covering the range of flow conditions to be studied. After the flume was oscillated at a constant rate for a period long enough to establish a natural bed shape, the flume was stopped and the bed dunes were measured. The bed shape was found to be approximately sinusoidal in the cross section under all flow conditions. The mean wavelength of the bed shape was 5.5 inches with a range of 4.5 to 8.0 inches; the mean wavelength-to-depth ratio was 8.0 with a range of 5.5 to 12. The fixed artificial roughness used approximates this shape. The artificial dunes were constructed of wood and fastened to a flexible sheet of plastic. Natural sediment with a mean diameter of 0.3 millimeter was glued to both the dunes and plastic. The plastic sheet was fixed to the flume bottom, covering the central 6.33 feet of the arc.

The asymmetric end roughnesses shown in Figure 1(c) were used to eliminate secondary currents in the central measuring section of the flume. Proper placement of the asymmetric roughness elements depends on the flow conditions of the flume. The optimum placement of the roughness elements for a given flow condition was determined by dropping potassium dichromate crystals through holes in the horizontal wave suppressent board and observing the movement of the dye streaks. When no transverse movement of the dye streaks in the central part of the flume were observed, the roughness elements were considered to be in the optimum location.

A lightweight, black plastic material with specific gravity of 1.25, which had been crushed and sieved, was used as artificial sediment in the experiments. The grain diameter of the sediments was uniform, bracketed by two consecutive sieve sizes of approximately the same diameter as the natural sediment glued to the flume bed. Only a small quantity of the sediment was used in the flume during an experiment in order to limit the deposition of sediment which would alter the flume bottom geometry.

When the sediment was first put into the flume it was found that air bubbles adhered to the sediment particles, thereby changing its settling velocity. To eliminate this buoyancy effect, deaerated water was used. The water was deaerated in a 60-cubic foot-capacity tank located on the wall of the laboratory at an elevation above the swing flume, heated by a 5-kilowatt immersion heater to a temperature of 90^{o} Fahrenheit, and then cooled to room temperature. The deaerated water was transported to the swing flume by gravity through a hose to reduce air entrainment.

The optical concentration meter used in the experiments was developed by Das (1971) for measuring *in situ* concentrations in laboratory flumes. The equipment consists of a light source, a beam collimator, a receiving unit, and necessary recording units. A collimated beam of light, 8.5-millimeter average diameter, is projected through the glass walls of the flume to a duo-photodiode mounted on the opposite side of the flume.

The photoelectric cell produces a signal which is proportional to the amount of light received which, in turn, is proportional to the amount of light blocked out by suspended sediment. The signal from the photoelectric cell is transmitted, amplified, and recorded on an analog paper chart recorder and an analog-to-digital data acquisition system set to sample at the rate of 58 samples per second. The light source and receiver are shown in Figure 2.

The light source and receiver are mounted on a rigid, aluminum yoke support (Fig. 3) held by friction brackets; by loosening four thumbscrews the elevation of the support can be varied from below the flume bottom to above the flume top while maintaining precise alinement of the optical equipment. This flexibility allows calibration of the optical equipment and flume concentration measurements to be made without removing the equipment from the supports. The yoke support and brackets are pinned to the laboratory ceiling on the same axis as the flume so that the optical equipment can swing with the flume or be held stationary in space.

2. Experimental Procedure.

a. Settling Velocity of the Sediment. The sediment used in the first series of experiments was the material which passed the 0.495-millimeter sieve and was retained on the 0.417-millimeter sieve. The fall velocity of this sediment was measured in a 2-inch-diameter glass cylinder filled with deaerated water at a temperature of 72° Fahrenheit. The time required for 220 particles chosen at random to fall 8.59 inches was measured with a stopwatch. The average settling velocity (V_s), the range of velocities, and the standard deviation were then calculated to be 0.035, 0.0213 to 0.0532, and 0.0059 foot per second, respectively.

b. Calibration of Optical Concentration Meter. Calibration of the optical equipment was done in a 0.5- by 0.5- by 1.0-foot clear, plastic calibration tank placed on the top of the swing flume. The 1.0-foot dimension of the tank was positioned parallel to the axis of the light source and receiver; i.e., the same width as the swing flume. The tank was then filled with a measured quantity of deaerated water. A small, measured amount of cleaned sediment was added to the tank and the sediment-water mixture was stirred mechanically to give a uniform suspended concentration. The collimated light beam and receiver were positioned and a 5-second record of the voltage from the receiver was recorded on the analog chart recorder and magnetic tape. Uniformity of concentration in the tank was checked by measuring the fraction of light blocked by the sediment at various locations in the cross section of the tank. The mechanical stirrer was stopped and the sediment allowed to settle. Records were then made of the voltage from the light beam passing through clear water and the voltage of the ambient light. The fraction of light passed was then calculated as the ratio of the voltage with sediment in suspension to the difference between the voltages of the beam through clear water and the ambient light. Measured amounts of sediment were

Figure 2. Optical concentration meter.

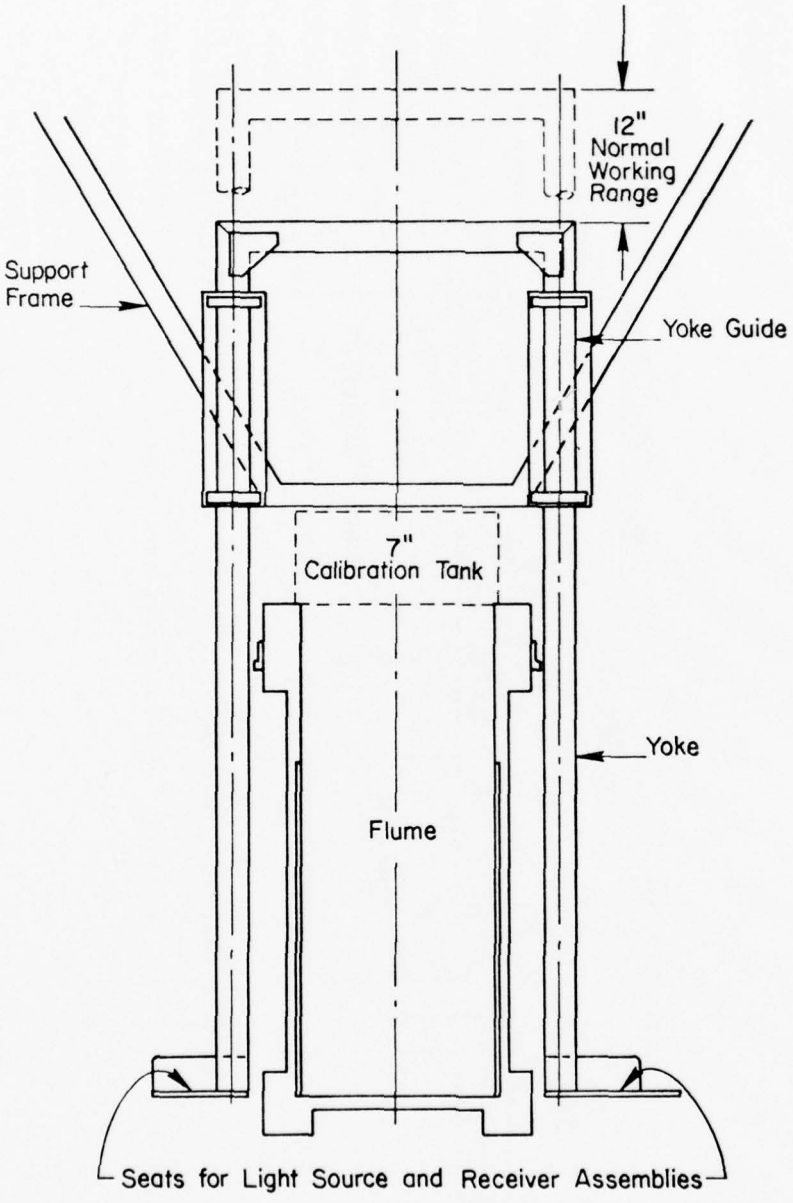

Figure 3. Yoke support for concentration meter.

added to the calibration tank and the procedure repeated until the range of the optical equipment was covered. Measurable concentrations ranged from 0.1 to 2.5 grams per liter. The logarithm of the fraction of light passed versus the concentration in grams per liter was plotted to give the calibration curve shown in Figure 4. The least squares, best fit equation for this curve is:

$$C = (-0.585)\ \ln_e[\bar{I}/(\bar{I}_o - \bar{I}')] \ , \qquad (8)$$

where

C = concentration (in grams per liter)

$\bar{I}$ = mean voltage from the receiver when the light beam is passed through the sediment-water mixture

$\bar{I}_o$ = mean voltage from the receiver when the light beam is passed through clear water

$\bar{I}'$ = mean voltage from the receiver when the light beam is turned off

The calibration curve, which was checked periodically during the experiments, did not change.

In setting up the calibration experiments, it was found that a change in the focus of the optical equipment would change the resulting calibration curve. To eliminate this problem a brace was made to hold the equipment in focus. A check of the focus was made during each concentration measurement by a wire-screen filter which, when placed in the light beam, blocked out a known and constant amount of light. If a change in focus was detected by the filter measurements, the concentration measurements were not used.

c. Concentration Distribution Measurements. For concentration distribution measurements in the flume, a datum elevation of the optical equipment had to be established. The mean elevation of the crest of the artificial dunes was used as the base elevation and was determined by a scale fixed to the flume and a pointer fixed to the optical equipment brace.

The desired period and eccentricity were selected and the flume linkage adjusted to give a symmetric oscillation. The flume was filled with deaerated water to the elevation of the wave suppressent board (12 inches above the lowest point of the bed), and the asymmetric end roughnesses were positioned. Depending on the flow conditions chosen, 100 to 500 grams of sediment was cleaned and deposited in the flume. The flume was then oscillated until the distribution of sediment in the flume was at equilibrium. The equilibrium condition was determined by periodically measuring the concentration of sediment at a fixed point in space until the concentration did not change with time.

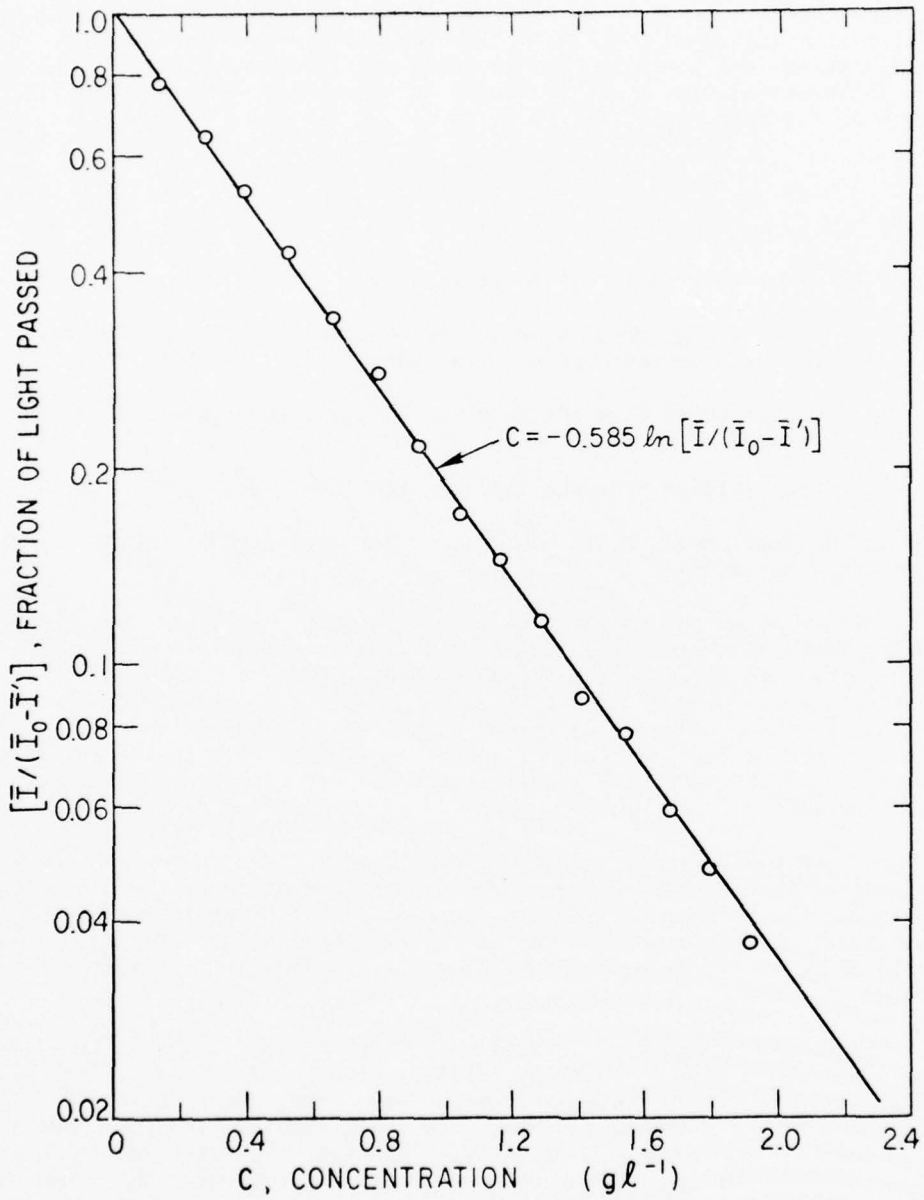

Figure 4. Calibration curve for sediment diameter: 0.417 millimeter $\leq$ D $\leq$ 0.495 millimeter, V_g = 0.035 foot per second.

The concentration distribution in the vertical was then measured for the flow condition selected. Again, for each elevation, voltage records were made for the sediment-laden water, clear water, ambient light, and clear water plus the filter. If the optical equipment was held stationary in space, the records for clear water and clear water plus filter were made while the flume was oscillated at such a long period that no sediment was in suspension. The time interval of the record for sediment-laden water, clear water, and clear water plus filter was always an integer multiple of the flume oscillation period. This procedure automatically allowed any irregularities in the transmissibility of the flume windows to be compensated for when calculating the fraction of light passed.

The output signal of the photoelectric cell, which was recorded on magnetic tape at the rate of 58 samples per second, was not constant with time, due to instantaneous concentration fluctuations. Because the concentration is related to the logarithm of the output voltage, it was necessary to calculate the concentration for each sample and then average the concentrations over the period of record to determine the true mean concentration.

The concentration measurements were usually started as near the boundary as possible, about 0.5 centimeter above the crest of the roughness elements. The flume was stopped, the elevation of the optical equipment was raised and recorded, and new measurements were taken. This procedure was followed until an elevation was reached at which the concentration was too low for the optical equipment to measure. The optical equipment was then lowered in a stepwise fashion until near the boundary to obtain concentration measurements at intermediate elevations. In this manner, 7 to 15 concentration measurements were obtained to describe the concentration distribution for one flow condition.

3. Results.

Sixty-five concentration distribution curves were obtained of the form,

$$C = C_o \exp(M\,Y) \quad , \tag{9}$$

where

M = slope of the curve (in feet^{-1})

C_o = concentration at the base elevation (in grams per liter)

C = concentration of sediment (in grams per liter); average of the concentrations calculated from equation (8) for each sample of record during the period

Y = elevation above the crest of the artificial roughness (in feet)

The variable used to describe the flow condition is the flow velocity, U_o, defined as:

$$U_o = (4\ L)/T\ , \qquad (10)$$

where L is the amplitude (in feet) and is equal to one-half the arc length which passes a fixed point during one-half cycle, and T is the period of oscillation (in seconds). The flow conditions studied ranged from a minimum of $U_o = 0.235$ foot per second (minimum to allow suspension of sediment) to a maximum of $U_o = 1.18$ feet per second (maximum allowed by flume construction). The amplitudes and periods used in these experiments ranged from 0.235 to 1.60 feet and 1.65 to 15.16 seconds, respectively. Figure 5 shows some typical concentration distribution curves that were obtained.

For the 65 different flow conditions studied, the base concentration, C_o (eq. 9), could not be correlated to any of the hydraulic parameters but depended on the amount of sediment in the flume. For different flow conditions the sediment in the flume would be distributed differently along the bottom of the flume, thereby giving a different and uncontrollable base concentration.

The 65 experiments also showed that two different laws exist in two ranges of conditions governing sediment suspension. For amplitudes of 0.693 foot and larger, the concentration distribution is determined by the flow velocity alone. For amplitudes less than 0.693 foot, the concentration distribution is a function of the amplitude relative to the wavelength of the artificial roughness.

Thirty-six of the 65 concentration distribution curves were determined using amplitudes of 0.693, 0.770, 0.925, 1.25, and 1.60 feet. For these five amplitudes, it was found that the slope of the distribution curve is a function of the flow velocity, independent of amplitude. Figure 6 graphically illustrates the relationship between M, the slope of the concentration distribution curve of equation (9), and U_o, the variable of equation (10) used to describe the flow conditions of the flume. These data are also tabulated in Table 1 which gives the periods, amplitudes, and use of the optical equipment. The least squares, best fit equation for this relationship is:

$$M = -18.45 + (11.53)\ U_o\ , \qquad (11)$$

where U_o is in feet per second, and M is the slope of the concentration distribution curve (in $feet^{-1}$). There is no statistical evidence to indicate that this relationship is significantly different from a higher order polynomial.

Results of experiments by Shinohara, et al. (1958) confirm the above results. They found the same linear relationship between the logarithm of concentration and elevation and qualitatively determined that as the intensity of the flow increased the slope of the concentration distribution curve, M, became flatter.

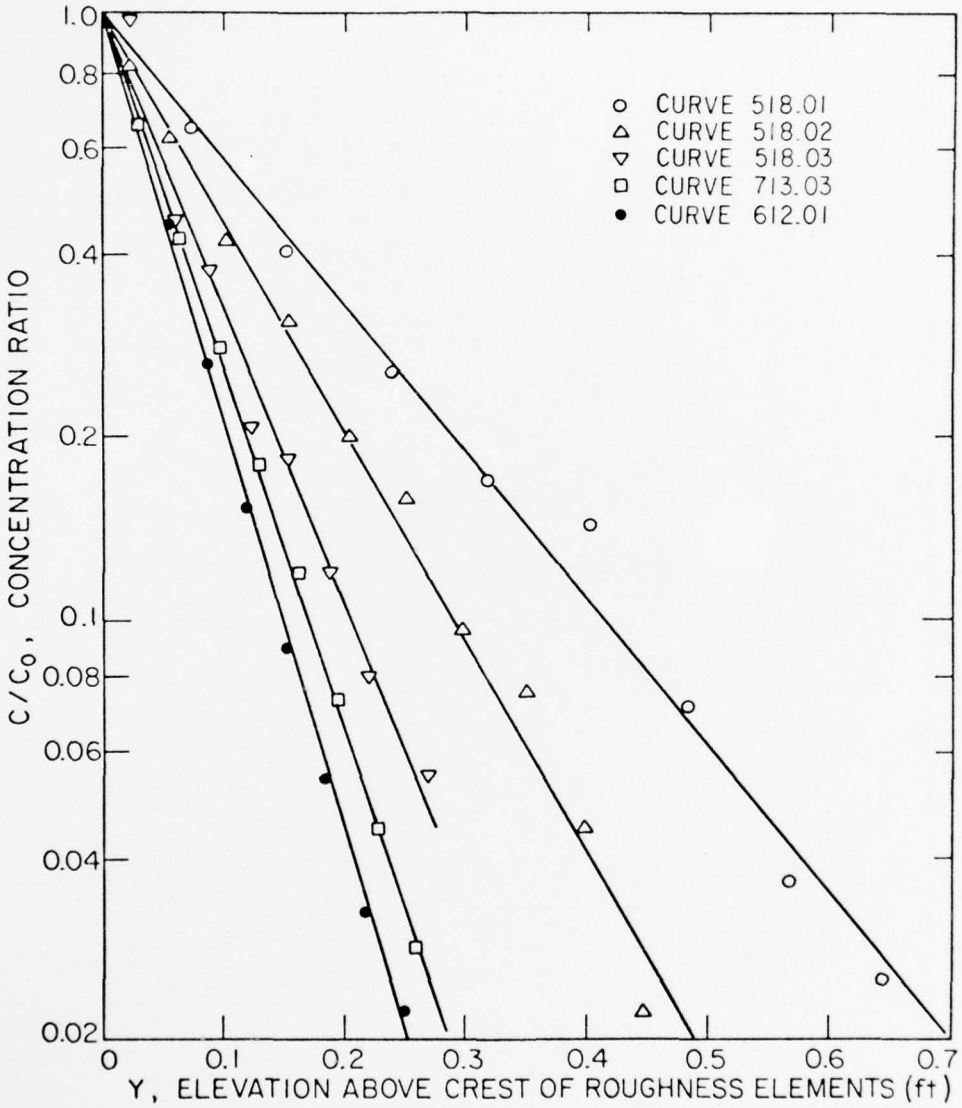

Figure 5. Examples of measured concentration distribution curves; sediment-settling velocity, V_s = 0.035 foot per second.

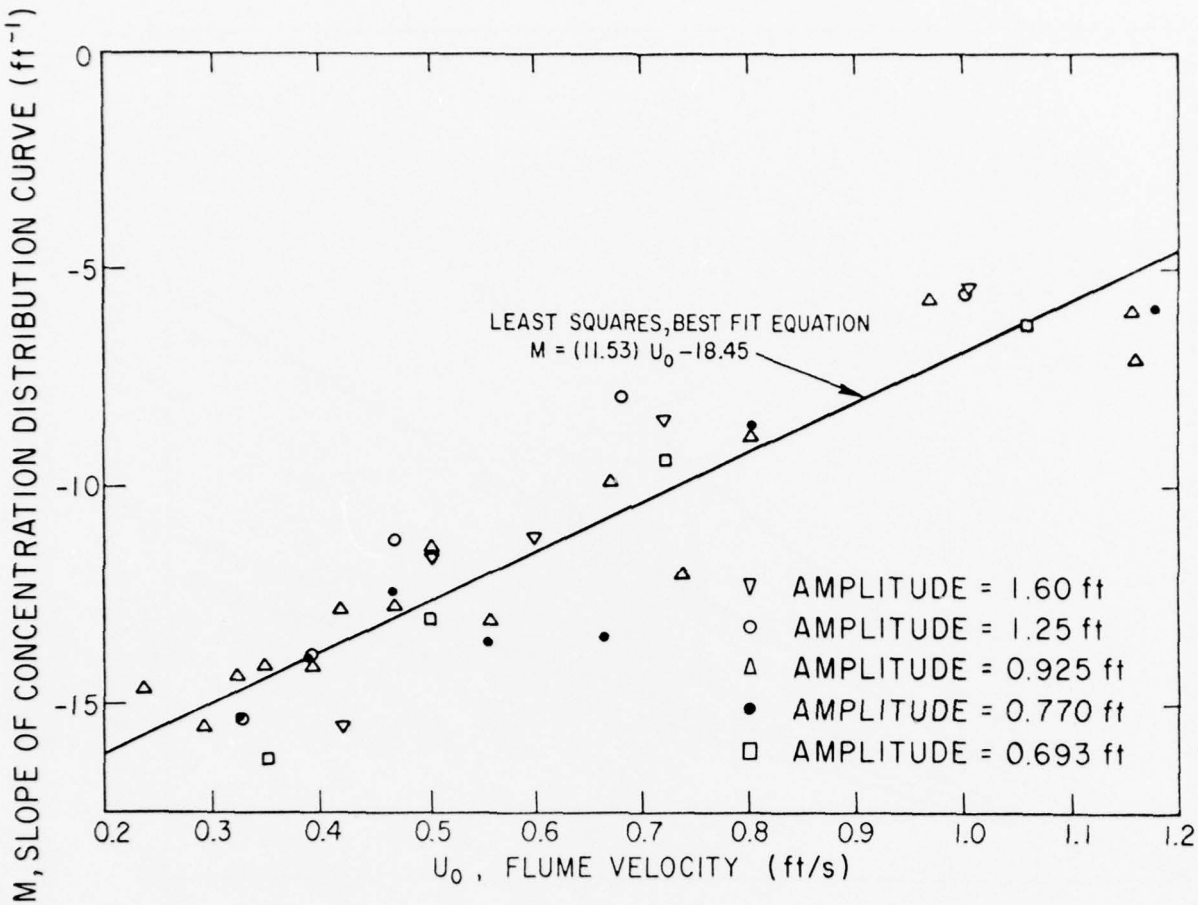

Figure 6. M versus U_o (eq. 4) for amplitudes equal to or greater than 0.693 foot and sediment-settling velocity, V_s = 0.035 foot per second.

Table 1. Concentration distribution data for V_s = 0.035 foot per second, amplitude ≥ 0.693 foot.

Curve No.	Period (s)	Amplitude (ft)	U_∞ (ft/s)	Slope, d(lnC)/d (ft^{-1})	Variance in least squares curve	Remarks
518.01	5.00	1.25	1.00	-5.60	0.0182	optics
518.02	7.34	1.25	0.681	-7.99	0.0184	stationary
518.03	10.63	1.25	0.470	-11.28	0.0196	
518.04	12.70	1.25	0.394	-13.91	0.0236	
518.05	15.16	1.25	0.330	-15.39	0.0136	
602.01	3.20	0.925	1.157	-5.96	0.0628	optics
602.02	5.02	0.925	0.737	-12.01	0.0140	stationary
602.03	7.34	0.925	0.504	-11.43	0.0151	
602.04	8.82	0.925	0.420	-12.90	0.00432	
602.05	10.61	0.925	0.348	-14.15	-------[1]	
602.06	12.63	0.925	0.292	-15.60	0.0170	
602.07	15.10	0.925	0.235	-14.67	0.0344	
612.01	15.14	1.60	0.422	-15.60	0.00386	optics
612.02	12.70	1.60	0.504	-11.66	0.0333	stationary
612.03	10.68	1.60	0.600	-11.20	0.0132	
612.04	8.88	1.60	0.721	-8.46	0.00359	
612.05	6.15	1.60	1.041	-5.45	0.0532	
705.01	3.19	0.925	1.16	-7.05	0.0189	optics
705.02	4.61	0.925	0.802	-8.88	0.00094	moving
705.03	6.60	0.925	0.560	-13.12	0.00120	
705.04	9.42	0.925	0.393	-14.20	0.00689	
707.01	3.82	0.925	0.968	-5.70	0.00798	optics
707.02	5.51	0.925	0.671	-9.92	0.00194	moving
707.03	7.87	0.925	0.470	-12.81	0.00333	
707.04	11.42	0.925	0.324	-14.44	0.00365	
713.01	2.61	0.770	1.18	-5.89	0.0422	optics
713.02	3.83	0.770	0.804	-8.58	0.00162	moving
713.03	5.52	0.770	0.558	-13.65	0.00113	
717.01	7.86	0.770	0.392	-13.95	0.0736	optics
717.02	9.39	0.770	0.328	-15.38	0.00946	moving
717.03	6.58	0.770	0.468	-12.43	0.0360	
717.04	4.62	0.770	0.667	-13.50	0.0202	
721.01	2.61	0.693	1.06	-6.29	0.00913	optics
721.02	3.83	0.693	0.723	-9.40	0.00236	moving
721.03	5.53	0.693	0.502	-13.10	0.00514	
721.04	7.88	0.693	0.352	-16.30	0.00320	

[1]Not calculated.

The same results were obtained more recently by Kennedy and Locher (1972). Their investigation examined the behavior of the mean sediment concentration and the periodic sediment concentration fluctuations. The experiments were conducted in a stationary flume with a fixed bed on which a limited amount of loose sediment was distributed. Turbulence for sediment suspension was caused by surface waves generated by a wave generator. The sediment concentrations were measured with optical equipment which incorporates the same theoretical principles as the equipment used in the swing-flume experiments but of a much smaller size. The smaller size and configuration of the equipment allowed measurements very near the bed and sampled a much smaller volume of flow.

Kennedy and Locher's (1972) experiments in mean sediment concentration distribution were limited to a wave height of 0.24 foot, a wave period of 1.0 second, and a mean water depth of 0.82 foot. The mean sediment concentration was measured at various elevations along five evenly spaced verticals in the flow. The spacing of the verticals was selected to cover one wavelength of the bed dune shape. A total of 78 data points was measured, and when the logarithm of the mean concentration was plotted against elevation above the bed a well-defined linear relationship of $C = C_o \exp(-36.5\ Y)$ was obtained. This relationship is identical to that obtained in the swing-flume experiments, with the exception of the high rate of decay of sediment concentration, (-36.5). Kennedy and Locher used a quartz sediment of 0.14-millimeter mean diameter in their experiments. The settling velocity of this sediment was not reported; it was probably about 0.050 foot per second, which is 43 percent greater than that of the principal plastic sediment (settling velocity of 0.035 foot per second) used in the swing-flume experiments. Swing-flume measurements, using sediments of different settling velocities, are discussed later in this section. For a given flow velocity a higher rate of decay of concentration is expected, as settling velocity increases.

Much of the analysis of data by Kennedy and Locher dealt with the periodic sediment concentration fluctuations. Although no specific conclusions were obtained regarding these fluctuations, the data did indicate the fluctuations were only apparent near the bed (within about 0.05 foot of the bed). This explains the lack of periodicity in concentration fluctuations for the swing-flume measurements, in that 0.05 foot is near the lower limit where the much larger optical equipment of the swing flume could be used.

Similar exponential concentration curves were obtained for the two different methods used in simulating sediment suspension in an oscillating flow; i.e., an oscillating flow over a fixed bed as used by Shinohara, et al. (1958) and Kennedy and Locher (1972), and an oscillating bed under a "stationary" body of water as used in the swing-flume experiments.

Figure 7 shows the relationship between M and U_o for two conditions. One set of data represents the condition that the optical equipment is stationary in space; the other data points are for the optical

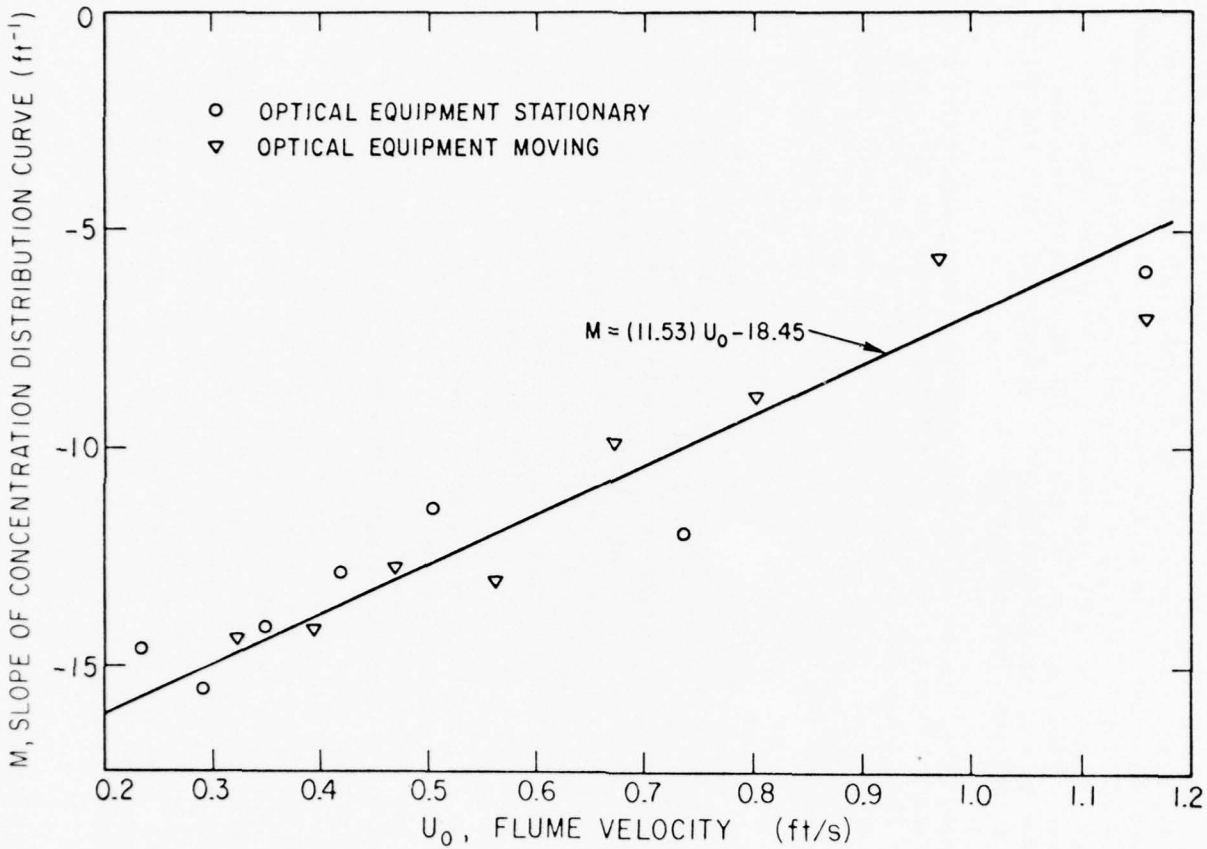

Figure 7. M versus U_o for optical equipment moving with the flume and stationary in space, using a 0.925-foot amplitude for all measurements; sediment-settling velocity, V_s = 0.035 foot per second.

equipment moving with the flume. All other variables in these experiments were the same. The amplitude of oscillation was 0.925 foot. There is no statistically significant difference in the results, indicating uniform suspension along the flume. None of the measurements for large amplitudes (greater than 0.925 foot) (Table 1) were made with the optical equipment moving with the flume. The reason for this is at large amplitudes the optical equipment would move into an area of the fluid where secondary circulations due to the asymmetric roughness elements may exist and therefore not give a representative concentration.

The remaining 29 of the 65 experiments were made using amplitudes of 0.235, 0.465, and 0.617 foot. Table 2 is a tabulation of the data, and Figure 8 shows the results of the 65 experiments. As shown in Figure 8, there is a great deal of scatter in the data for small amplitudes; therefore, only qualitative conclusions have been made. In general, the smaller the amplitude the smaller the slope of the concentration distribution curve.

Experiments, movies, and photos were used to determine why the small amplitudes do not obey the flow velocity relationship of the larger amplitudes given in equation (11). Based primarily on visual observation, the following explanation is hypothesized. For small amplitudes, the distance of travel of the flume bottom during a half cycle is not great enough for the boundary layer to fully develop during each stroke and to become turbulent. Only at the end of the half cycle when the acceleration forces cause separation is sediment thrown into suspension. Separation only occurs at the downstream face of the artificial dunes. The observed suspension pattern when a 0.235-foot amplitude of oscillation was used consisted of plumes of suspension separated by areas of zero concentration. These plumes were accentuated because, on the return, the half-cycle separation at the downstream face occurred such that the succeeding burst of sediment was thrown into approximately the same region of fluid as in the first half cycle; i.e., the amplitude of motion was about equal to a multiple of the wavelength of the dune shape. When the amplitude was increased to 0.465 foot, a more fully developed boundary layer was attained. In this case, separation occurred over a somewhat longer distance of travel but still less than the wavelength of the dune shape because less deceleration force was required. The suspension pattern was the same as with the 0.235-foot amplitude but much less distinct; the plumes were wider and overlapping. Finally, with the 0.693-foot amplitude, separation occurred over a distance equal to or greater than the wavelength of the dunes, and a uniform longitudinal concentration was attained.

Special experiments were conducted to verify the above hypothesis. The vertical distribution of concentration at various horizontal locations in the fluid was measured to determine if the concentration distribution varied. If the above hypothesis is correct, the concentration distribution should vary along the horizontal and in a regular manner determined by the shape of the bed dunes. In addition, if suspension

Table 2. Concentration distribution data for V_o = 0.035 foot per second, amplitude < 0.693 foot.

Curve No.	Period (s)	Amplitude (ft)	U_o (ft/s)	Slope d(lnC)/d (ft^{-1})	Variance in least squares curve	Remarks
621.01	2.11	0.617	1.170	-11.15	0.0511	optics
621.02	3.18	0.617	0.777	-16.15	0.0459	stationary
621.03	4.60	0.617	0.537	-13.10	0.0134	
621.04	6.58	0.617	0.375	-15.12	0.00268	
621.05	9.38	0.617	0.263	-10.95	0.0233	
628.01	9.40	0.617	0.263	-16.63	0.00522	optics
628.02	6.57	0.617	0.376	-16.50	0.00247	moving
628.03	4.59	0.617	0.538	-17.30	0.0305	
629.01	3.17	0.617	0.780	-13.20	0.00778	optics
629.02	2.10	0.617	1.177	-11.50	0.00776	moving
629.03	2.61	0.617	0.947	-9.50	0.00753	
629.04	5.51	0.617	0.448	-15.53	0.00858	
711.01	1.67	0.465	1.113	-10.16	0.0247	optics
711.02	2.60	0.465	0.715	-13.21	0.00401	moving
711.03	3.82	0.465	0.487	-16.63	0.00631	
711.04	5.51	0.465	0.337	-20.33	0.00885	
711.05	4.60	0.465	0.405	-23.27	0.0157	
711.06	3.19	0.465	0.583	-19.00	0.00766	
711.07	2.09	0.465	0.890	-30.10	0.0262	
802.01	1.65	0.235	0.570	-43.35	0.0150	optics
802.02	2.08	0.235	0.452	-29.60	0.0204	moving
802.03	2.59	0.235	0.363	-31.05	0.0292	
802.04	3.81	0.235	0.247	-43.50	0.00577	
802.05	3.17	0.235	0.297	-45.10	0.00821	
814.01	3.18	0.465	0.585	-17.20	0.00481	optics
814.02	3.18	0.465	0.585	-14.10	0.0239	stationary
814.03	3.18	0.465	0.585	-12.82	0.0208	
814.04	3.18	0.465	0.585	-15.72	0.0152	
814.05	3.18	0.465	0.585	-14.00	0.0447	

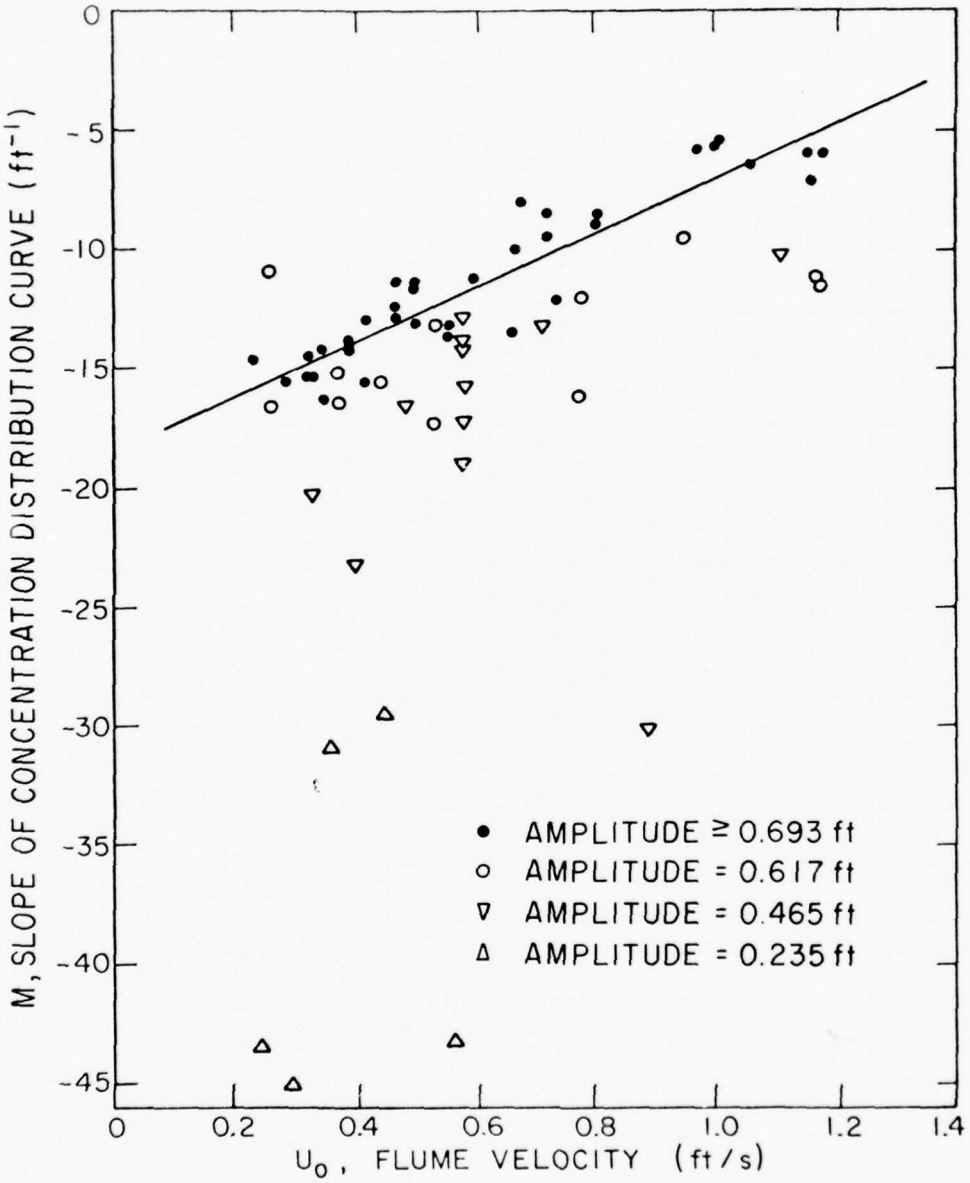

Figure 8. M versus U_o for sediment-settling velocity, V_s = 0.035 foot per second.

for small amplitudes is a function of location, the shape of the concentration distribution curve for a particular vertical may not be the same flume velocity, U_o, but with a large amplitude. The following is a description of the experiments.

The flume was adjusted to a 0.465-foot amplitude and a 3.18-second period was selected. A special brace with attached scale was constructed to hold the optical equipment stationary in space, and therefore stationary relative to the fluid. This brace allowed relocation of the optical equipment to any desired new location along its arc while maintaining the freedom to change the elevation of the optical equipment relative to the bed of the flume. An initial location of the optical equipment was chosen and a vertical concentration distribution measured. The optical equipment was then relocated to a new position and another concentration distribution was measured. This procedure was repeated until five concentration distribution curves were obtained. Each was at a different horizontal location relative to the position, at a fixed phase, of the flume bed, but with identical flow conditions of the flume. The horizontal range of the five distribution curves was about equal to one wavelength of the bottom roughness shape. The results of these experiments (Fig. 9) indicate that the distribution of concentration is not uniform along the flume bed for the 0.465-foot amplitude studied. Figure 9 also indicates that the rate of sediment concentration decay is less in the areas between the dunes and greatest at the crest of the dunes. This implies that the plumes of suspension are above the trough of the bed shape, where it would be expected if the sediment is thrown upward and downstream from the downstream face of the dunes.

Figures 10 to 14 are the concentration distribution curves measured for the locations indicated in Figure 9. Although not conclusive, these data indicate that the vertical distribution of sediment in the plumes does not conform to the exponential distribution of equation (9). The relationships shown in Figures 11 to 14 display a slight, but statistically significant curvature and were obtained at locations in the plume; whereas, Figure 10 shows no curvature and was obtained at a location between plumes. This could be explained by the existence of periodic stationary eddies, one located on each side of the plume axis. The eddies would sweep sediment into the base of the plume axis giving a relatively high concentration and carry sediment out of the top of the plume, causing the concentration to be lower than would be predicted in a randomly turbulent flow field.

The small amplitudes studied represented rare prototype conditions; therefore, all subsequent experiments were limited to amplitudes greater than 0.617 foot.

4. Experiments Using Sediments of Different Settling Velocities.

Two different sediments of the same black plastic were selected and investigated to determine the effect of settling velocity on the

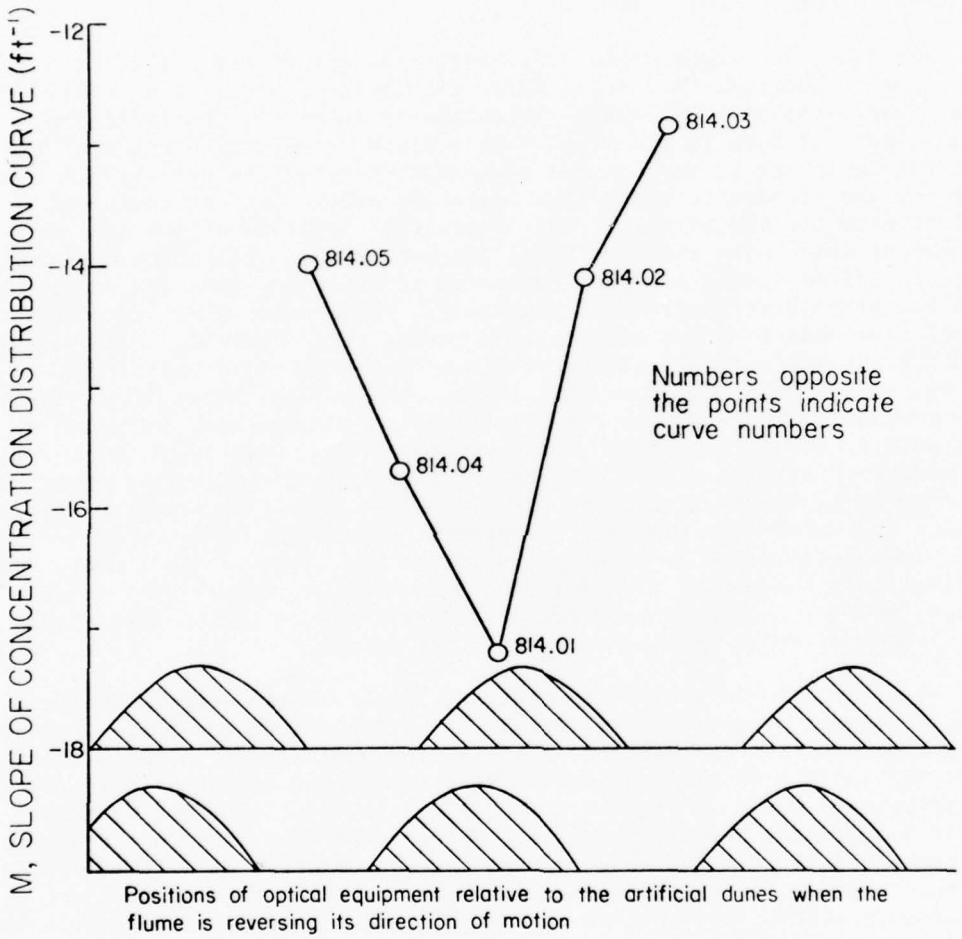

Figure 9. M versus location of optical equipment for identical flow conditions, V_s = 0.035 foot per second.

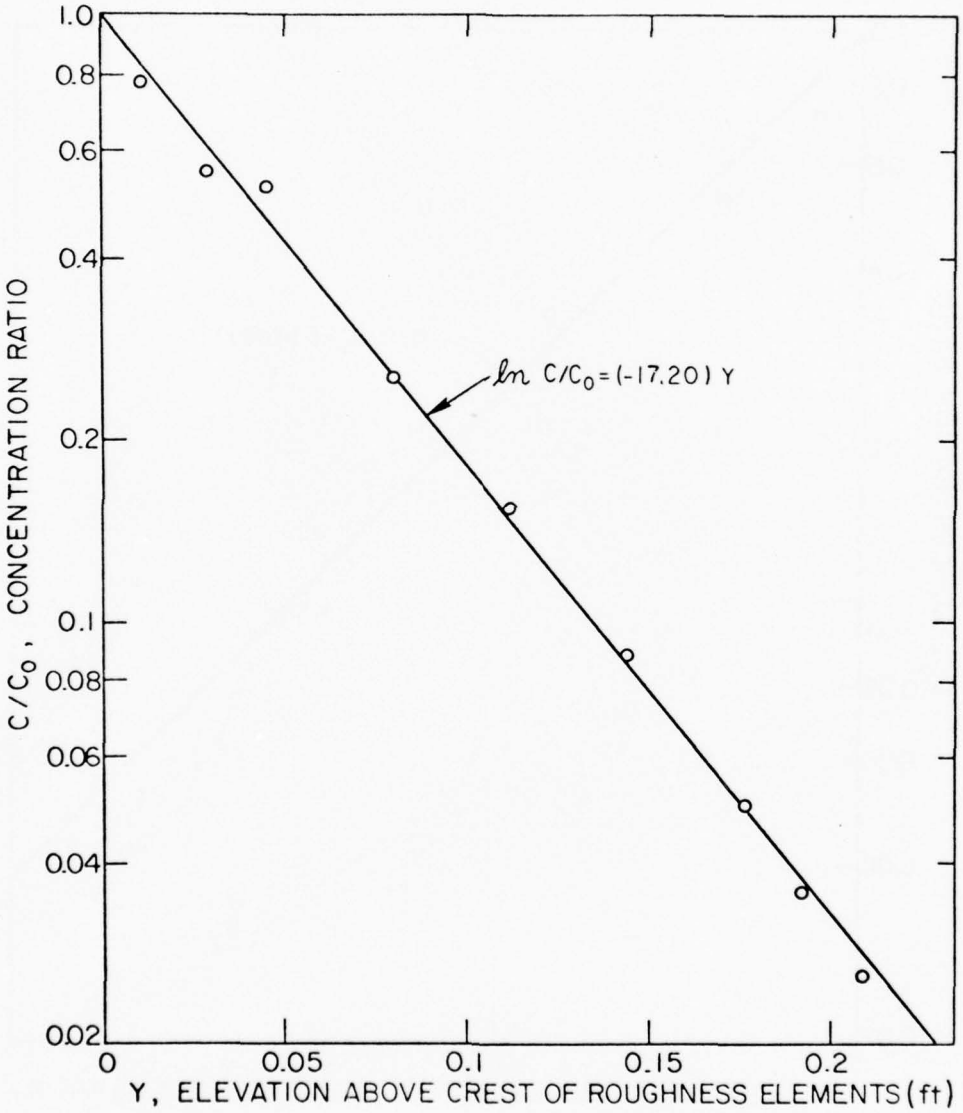

Figure 10. Concentration distribution for run 814.01.

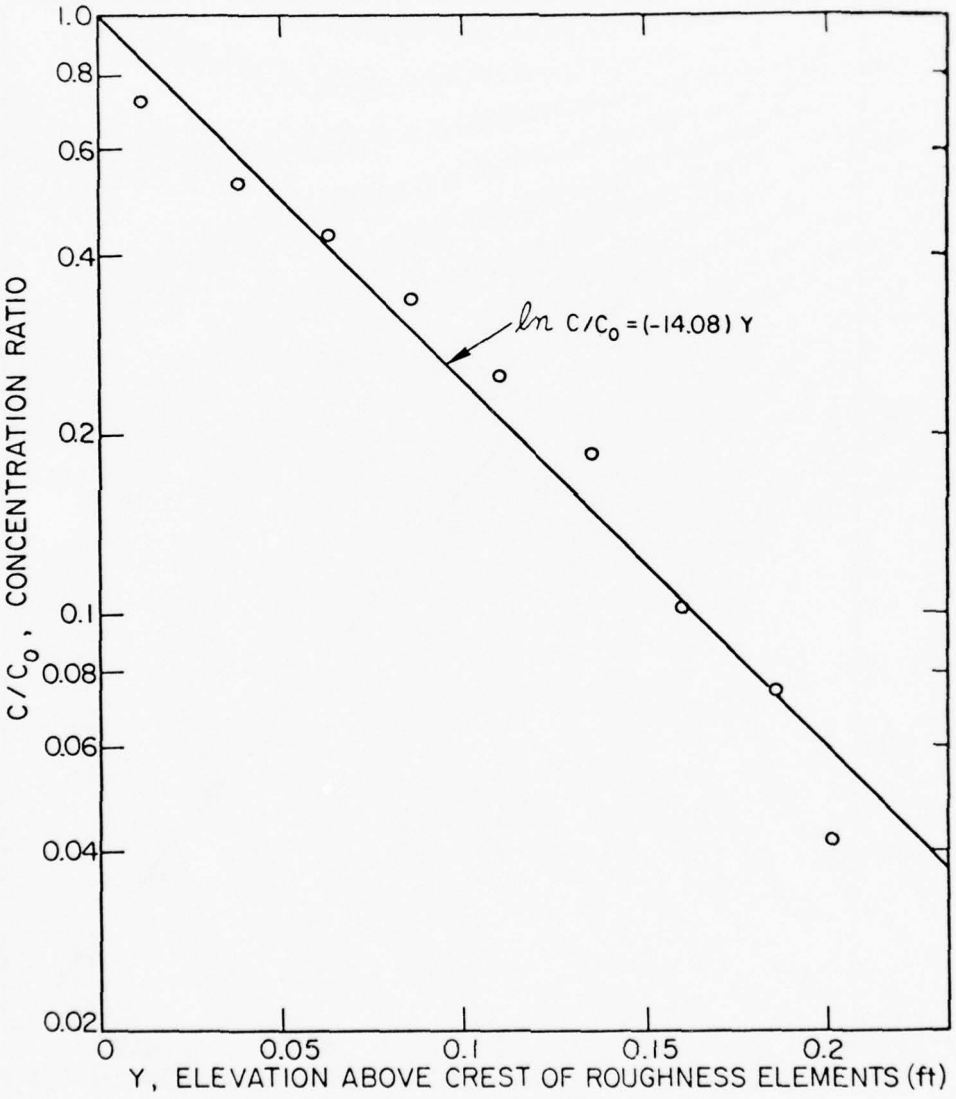

Figure 11. Concentration distribution for run 814.02.

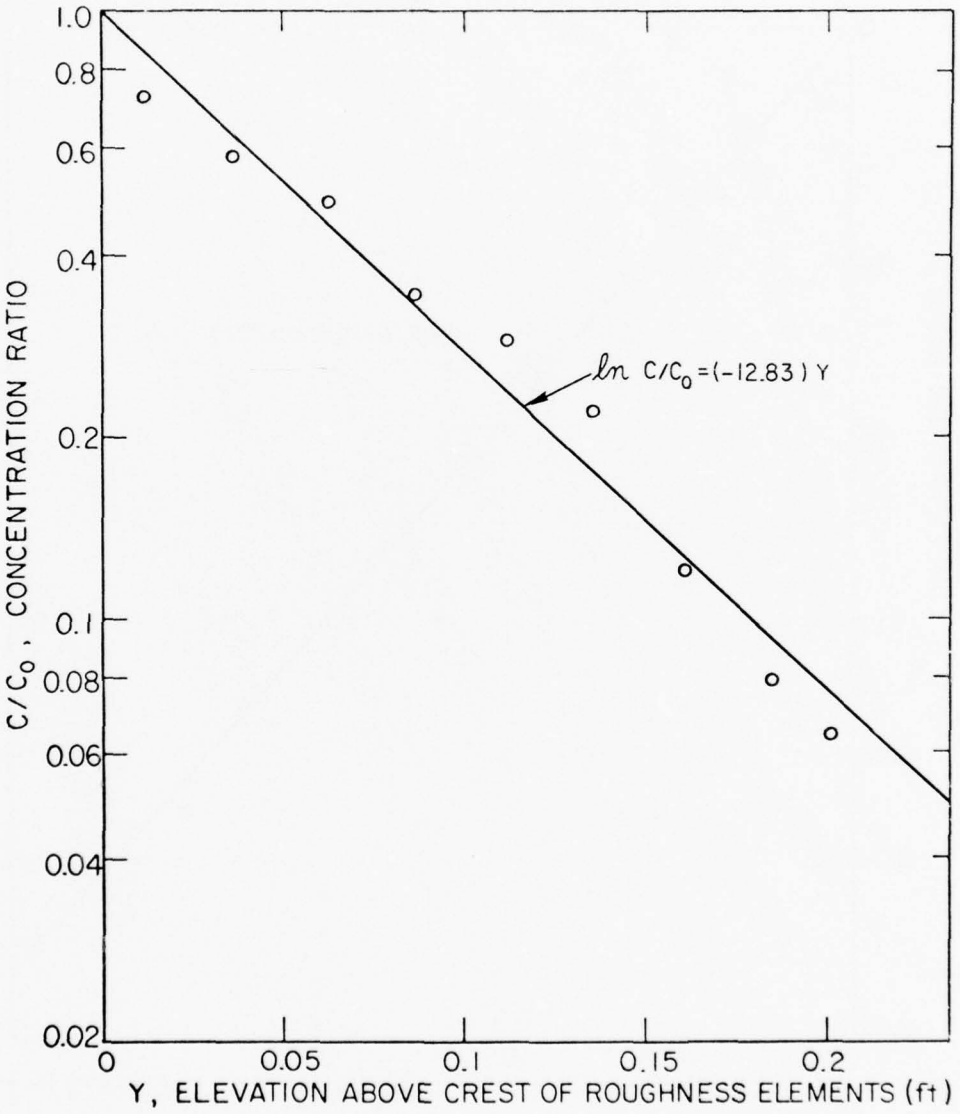

Figure 12. Concentration distribution for run 814.03.

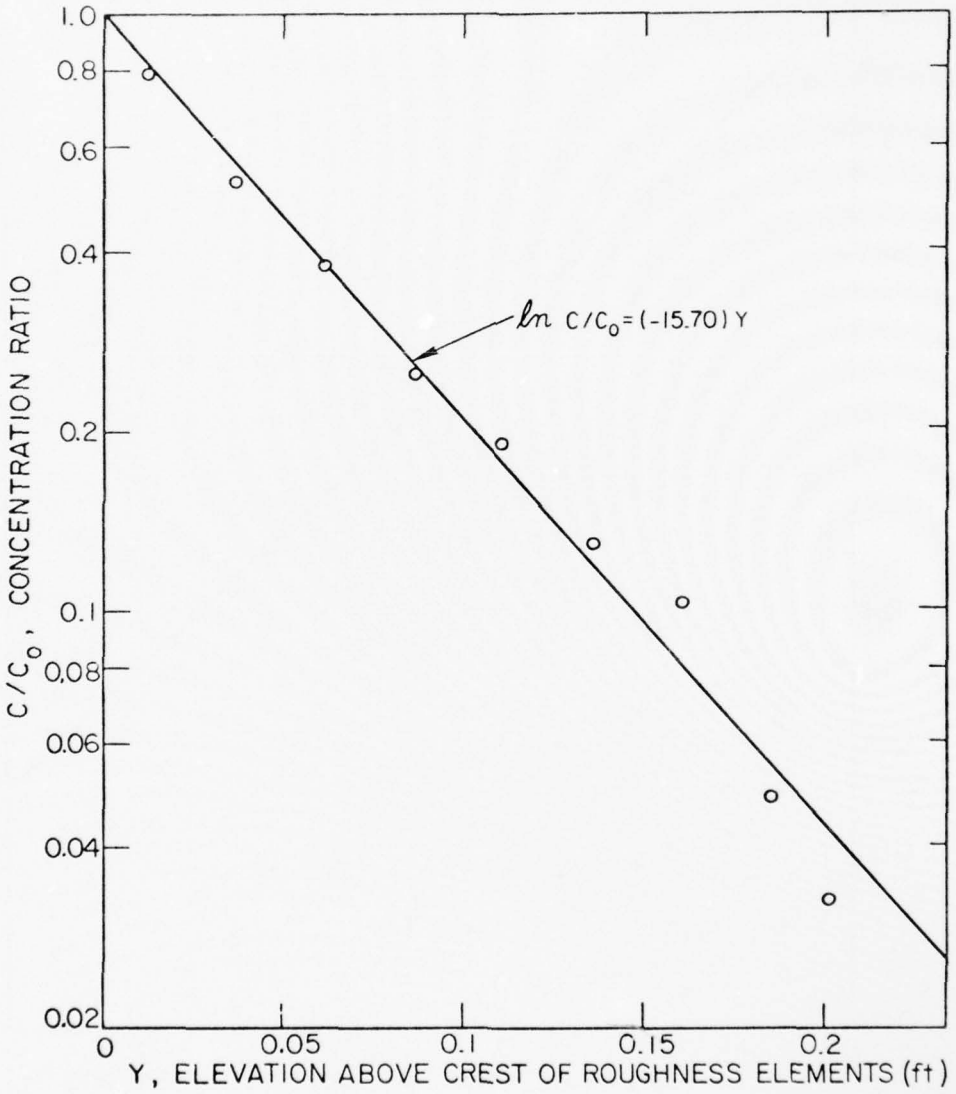

Figure 13. Concentration distribution for run 814.04.

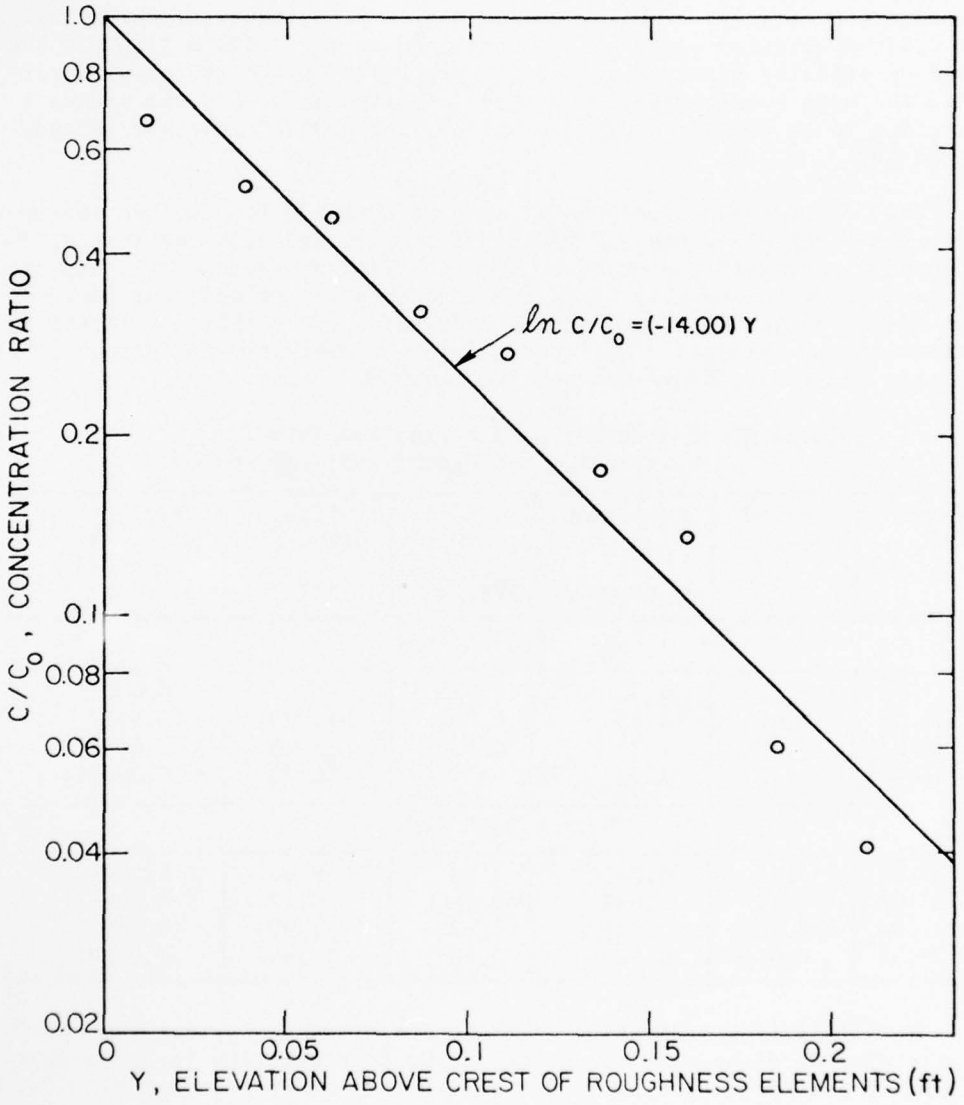

Figure 14. Concentration distribution for run 814.05.

concentration distribution. The first of these sediments was the material which passed the 0.701-millimeter sieve and was retained on the 0.589-millimeter sieve. Settling-velocity measurements of 225 randomly chosen particles determined the mean settling velocity, the velocity range, and the standard deviation as 0.0626, 0.0387 to 0.113, and 0.0131 foot per second, respectively. The second sediment was the material which passed the 0.589-millimeter sieve and was retained on the 0.495-millimeter sieve. Settling-velocity measurements of 240 particles of this material determined the mean settling velocity, the velocity range, and the standard deviation to be 0.0498, 0.0285 to 0.0754, and 0.00885 foot per second, respectively.

Table 3 gives the experimental results obtained for the two sediment types and Figure 15 shows how these results compare with the results for sediment with a settling velocity of 0.035 foot per second. As expected, for sediment with a higher V_s, the concentration of sediment decreases with elevation above the bed at a higher rate. Only this qualitative conclusion was obtained. Not enough data were obtained to define quantitatively the relationship between V_s and M.

Table 3. Concentration distribution data for V_s = 0.0626 and 0.0498 foot per second.

Curve No.	Period (s)	Amplitude (ft)	u_o (ft/s)	*Slope*, d(lnC)/d (ft^{-1})	*Variance in* least squares curve
V_s = 0.0626 ft/s					
913.01	4.62	1.25	1.082	-6.02	0.0327
913.02	6.60	1.25	0.758	-11.90	0.0154
913.03	9.43	1.25	0.530	-15.68	0.00497
913.04	11.46	1.25	0.437	-16.72	0.000966
V_s = 0.0498 ft/s					
927.01	3.14	0.848	1.08	-6.96	0.00095
927.02	3.99	0.848	0.850	-9.77	0.00698
927.03	4.98	0.848	0.682	-11.90	0.00378
927.04	6.08	0.848	0.558	-12.80	0.00177

The interesting indication of these measurements is that the increase in the rate of decay with elevation of the concentration for a sediment of higher settling velocity is not as great as predicted from the O'Brien (1933) equation for concentration equilibrium conditions. Consider the concentration equilibrium equation used in unidirectional flow for suspended sediment:

$$C\,V_s + E(dC/dY) = 0\ , \qquad (12)$$

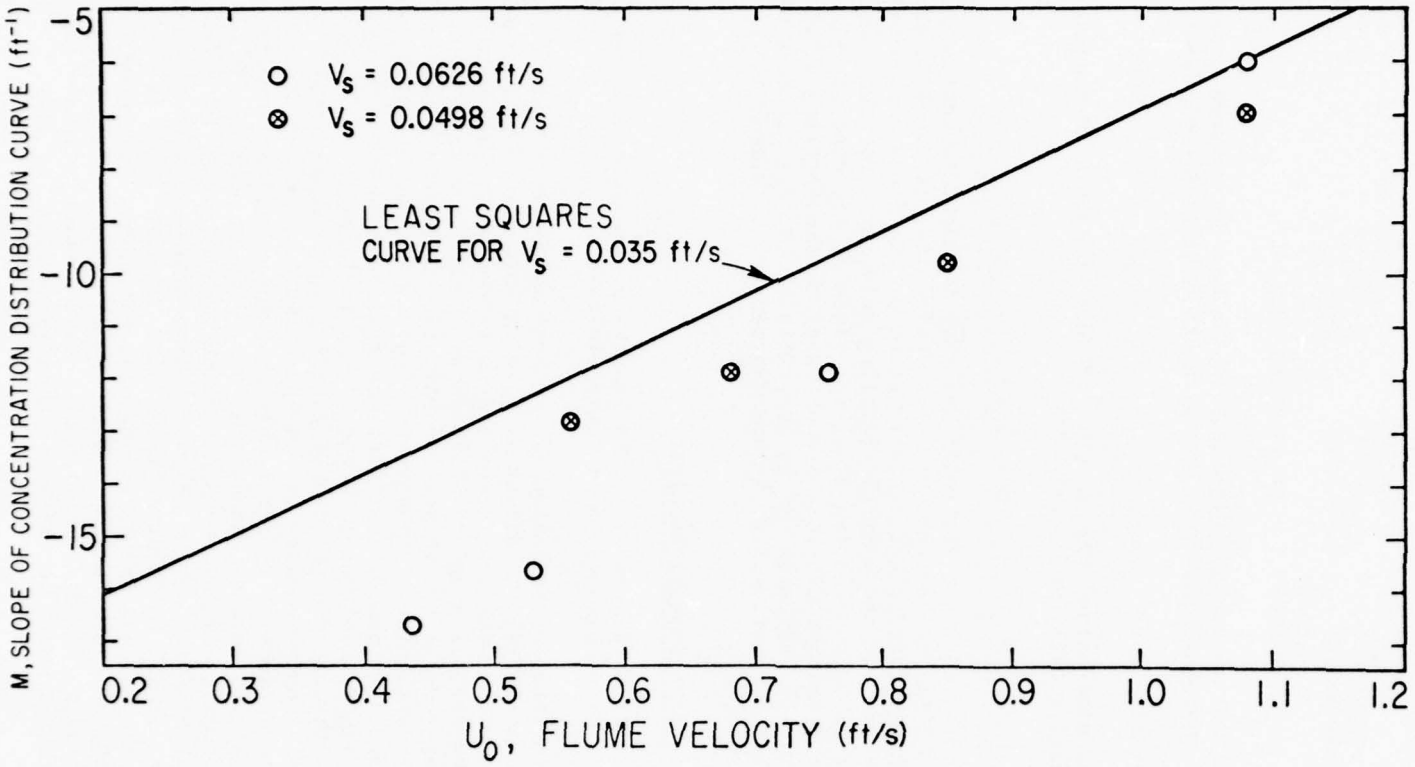

Figure 15. M versus U_o for V_s = 0.035, 0.498, and 0.0626 foot per second.

where

C = concentration

V_s = settling velocity of the sediment particle

E = sediment exchange coefficient (which here is assumed equal to the momentum exchange coefficient in unidirectional flow)

Y = elevation above the bed

Inserting the expressions for C and (dC/dY) obtained from equation (9) into equation (12) and solving for E yield:

$$E = -V_s/M \ . \tag{13}$$

In unidirectional flow and for relatively low sediment concentrations, it is assumed that the sediment exchange coefficient is equal to the momentum exchange coefficient, is a function of the fluid motion only, and is independent of the particle-settling velocity. For this assumption to be valid in oscillating flow, the slope of the concentration distribution curve must be directly proportional to the settling velocity. Although Figure 15 indicates M is proportional to V_s, it does not indicate direct proportionality. This discrepancy is discussed in Section IV.

5. Summary of Experimental Results.

The following is a summary of the results of the concentration measurements and a brief discussion of their limitations.

a. The vertical distribution of sediment concentration can be expressed by equation (9). Sediment is held in suspension by the random motion of turbulence which is generated in the boundary layer and is transported by diffusion upward while decaying continuously because of viscosity. As shown later in Section III, the turbulence intensity decays rapidly with elevation above the bed. The upper elevation to which the turbulence can diffuse (the water surface in the prototype and the wave suppressent board in the flume) is larger than the elevation at which the turbulence intensity decays to extremely small values; therefore, this upper boundary can be approximated as being at infinity. Under these conditions it is reasonable that the empirical results given by equation (9) indicate an exponential decay (as is commonly found in a diffusion process), and only become zero at Y = infinity. As expected, the concentration distribution in oscillating flow is different than in unidirectional flow. In unidirectional flow the turbulence is distributed between the bed and the water surface, the turbulence intensity is significant at the water surface. Because the water surface is not effectively at infinity, the distribution of both the turbulence and the sediment concentration would be different than in oscillating flow.

b. The base concentration, C_o (eq. 9), for flume measurements is a function of the sediment charge in the flume and therefore could not be correlated to flow hydraulics. As shown by Einstein (1950), a flow is only capable of transporting a limited amount of sediment of a given size. This limiting capacity is determined by the flow velocity, sediment characteristics, and roughness of the boundary. In addition, the flow will only transport this capacity rate if there is a sufficient supply of sediment available. Otherwise, the transport rate will be reduced by the ratio of the supply rate to the capacity rate. Because the capacity transport rate for a given flow is determined by the probability of a particular sediment particle being subjected to sufficient hydraulic forces to move it, there must be some particles in the bed that are not in motion at any instant of time. Had there been enough sediment in the flume to satisfy the flow's sediment transport capacity, the measured C_o could have been correlated to flow velocity. Unfortunately, under those conditions some sediment must be loosely deposited on the flume bed, thereby changing the fixed-bed geometry and roughness. Therefore, only the flow's capacity to transport sediment of a specific size can be estimated. This estimate must use the capacity base concentration calculated from Kalkanis' (1964) bedload equation and not the base concentrations measured in this investigation.

c. In the range of flow velocities, 0.2 foot per second $< U_o <$ 1.1 feet per second, for amplitudes of oscillation equal to or greater than 0.693 foot, and for V_g = 0.035 foot per second, the slope of the exponential distribution of sediment concentration is a function of flow velocity only. The slope, M, can be approximated from the flow velocity, U_o, by equation (11). This equation is only a best fit empirical relationship and cannot give reasonable approximations of M for U_o values very far outside the stated range. This becomes apparent when substituting in a large value of U_o; e.g., 2.0 feet per second, and calculating M. The result would be a positive value for M; i.e., the concentration of sediment increases with elevation which is not reasonable. The limiting value of M for extremely large values of U_o should be zero, or uniform concentration of sediment throughout the depth. At the other extreme, equation (11) gives a value of M = -18.45 feet^{-1} for U_o = 0 foot per second which is also not reasonable. But, for low values of U_o, any continuous function is not expected to give a correct relationship since at some point the flow changes from turbulent to laminar. In laminar flow there is no turbulence and therefore no sediment suspension. As U_o is increased, the flow, at some velocity, suddenly changes from laminar to turbulent and just as suddenly the suspended-sediment concentration changes from zero to some positive value. Therefore, the relationship expressed by equation (11) becomes invalid at some small value of U_o.

d. For the flow velocities studied, the sediment-settling velocity has a significant effect on the slope of the concentration distribution curve. Not enough data were obtained to define the relationship between V_g and M, but the data did yield the qualitative relationship that for constant U_o, M decreases (or becomes a larger negative value) with increasing V_g. As discussed earlier, if the sediment exchange coefficient

is equal to the momentum exchange coefficient, as is assumed for unidirectional flow, the slope, M, should be directly proportional to V_s. The experimental results for oscillating flow did not indicate direct proportionality. Therefore, the sediment exchange coefficient for oscillating flow given by equation (13) is, as yet, an undetermined function of V_s and U_o. A discussion in Section IV indicates why this result is expected.

III. DISTRIBUTIONS OF TURBULENT VELOCITY FLUCTUATIONS

1. Experimental Apparatus.

Successful measurements of turbulent velocity fluctuations in fluids have been made using either constant current or constant temperature hot-film anemometers. A constant temperature, quartz-coated hot-film sensor, model number 6010 made by Thermo-Systems Incorporated, Minneapolis, Minnesota, was used in this investigation. The sensor was connected to a 1050 series anemometer also made by Thermo-Systems Incorporated. The anemometer uses a bridge and feedback system to maintain a constant resistance and therefore a constant temperature of the sensor. Any change that affects the heat transfer between the sensor and the environment is reflected in the voltage output of the bridge. This output voltage is amplified and recorded on magnetic tape. The record of voltage fluctuations is then converted by use of a calibration curve to a record of velocity fluctuations. A schematic of the hot-film bridge is shown in Figure 16. The hot-film sensor and probe are shown in Figure 17.

Calibration of the hot-film anemometer was done in the calibration tank (Fig. 18) which was divided into two chambers, a fore chamber and a calibration chamber. The fore chamber contained two wire screens to ensure a uniform velocity distribution. The two chambers were connected by a 1-inch-diameter nozzle located at the midpoint of the partition separating the two chambers, 5.25 inches above the bottom of the tank. An overflow was located at the downstream end of the calibration chamber, 4.75 inches above the nozzle. Water was supplied from the deaeration tank, the rate controlled by a 0.25-inch needle valve. The flow into the calibration chamber was a submerged jet. The probe with sensor was held at the downstream face of the nozzle by clamps connected to a point-gage assembly. The point-gage assembly was used to raise and lower the sensor known amounts to obtain velocity measurements across the diameter of the nozzle. The water collected at the overflow in a measured time was weighed to determine the flow rate and mean nozzle jet velocity.

Measurements of the turbulent velocity distributions were conducted in the swing flume. Only minor modifications to the flume apparatus were necessary to accommodate the anemometer equipment.

As shown in Figure 17, the sensor is extremely delicate and therefore cannot be used in flows containing solid particles. For this reason the flume had to be cleaned of all the black plastic sediment used in

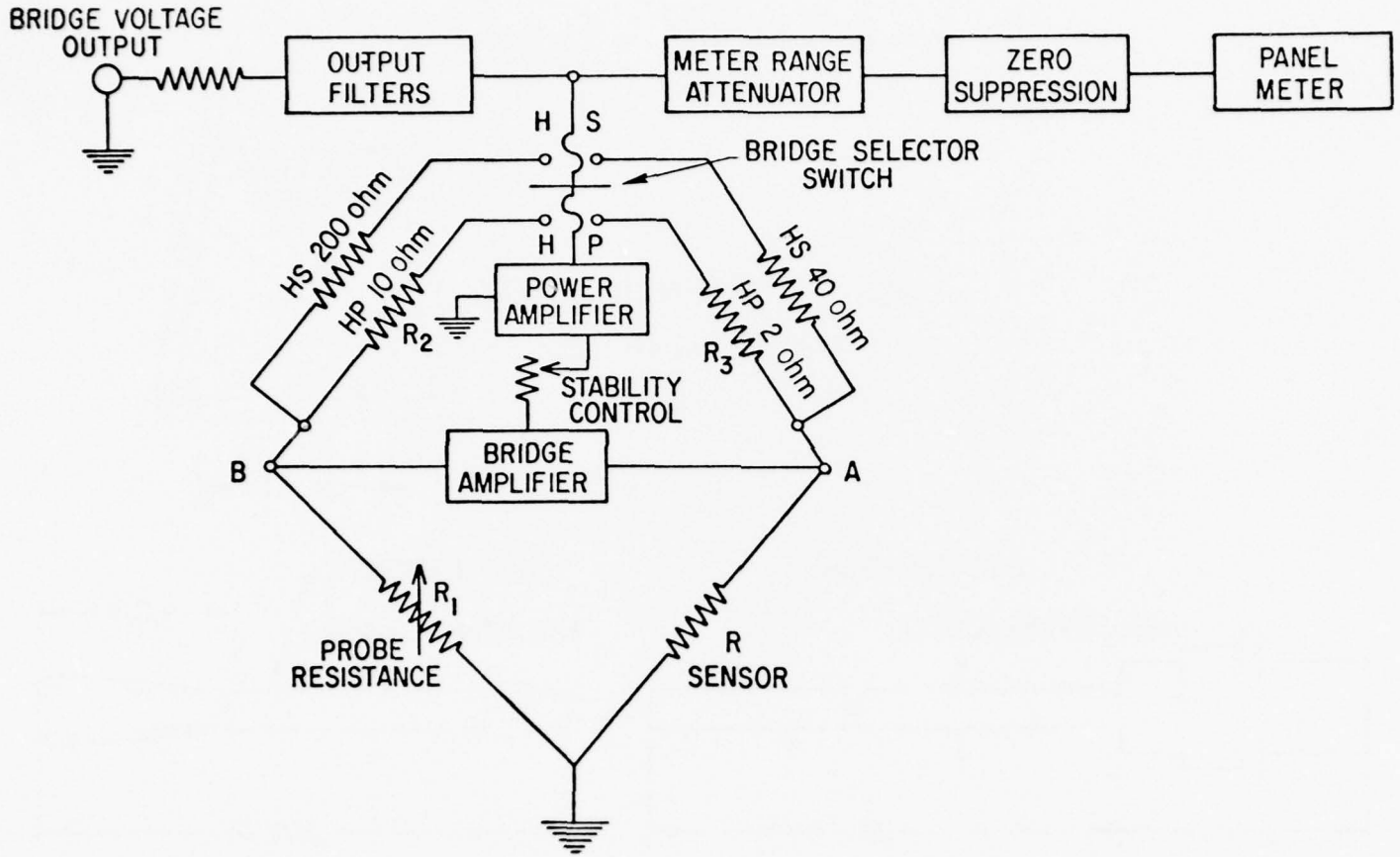

Figure 16. Functional schematic of hot-wire bridge circuit.

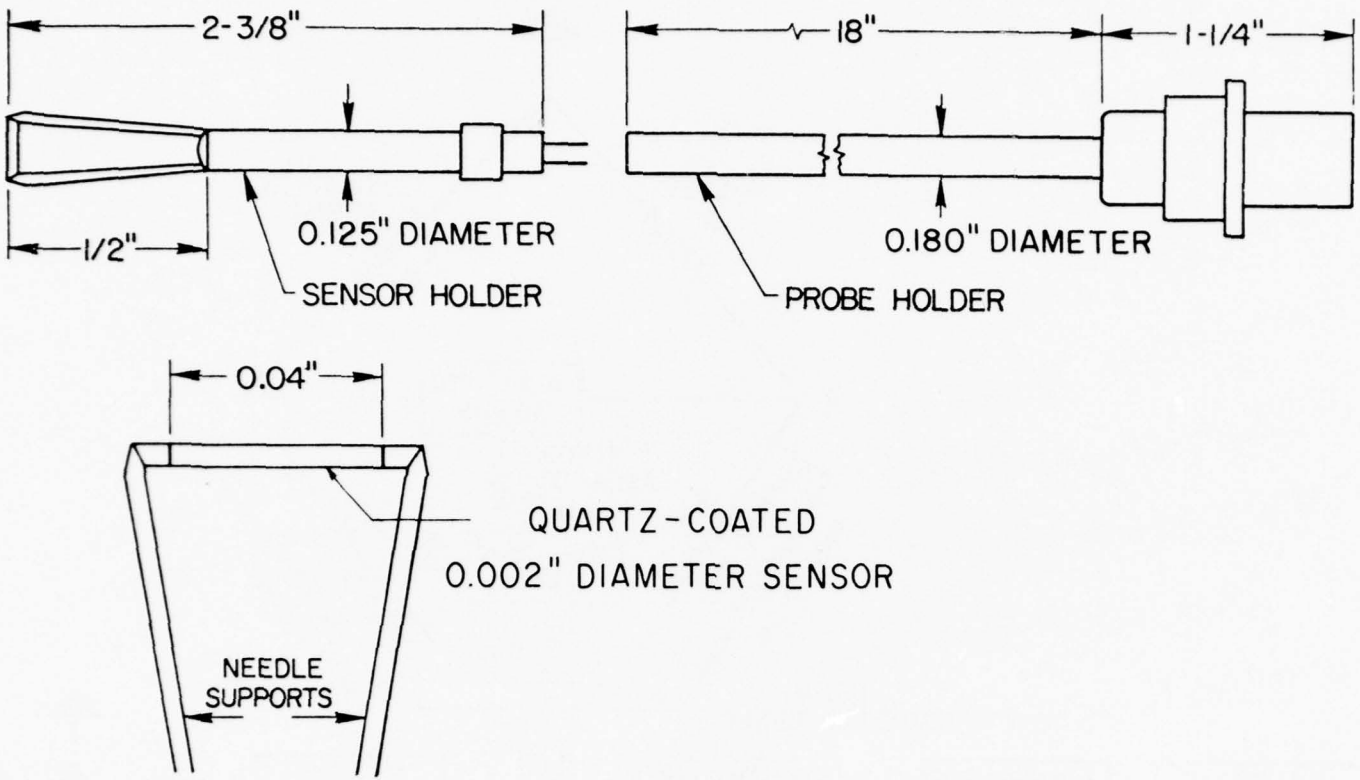

Figure 17. Hot-film sensor and probe.

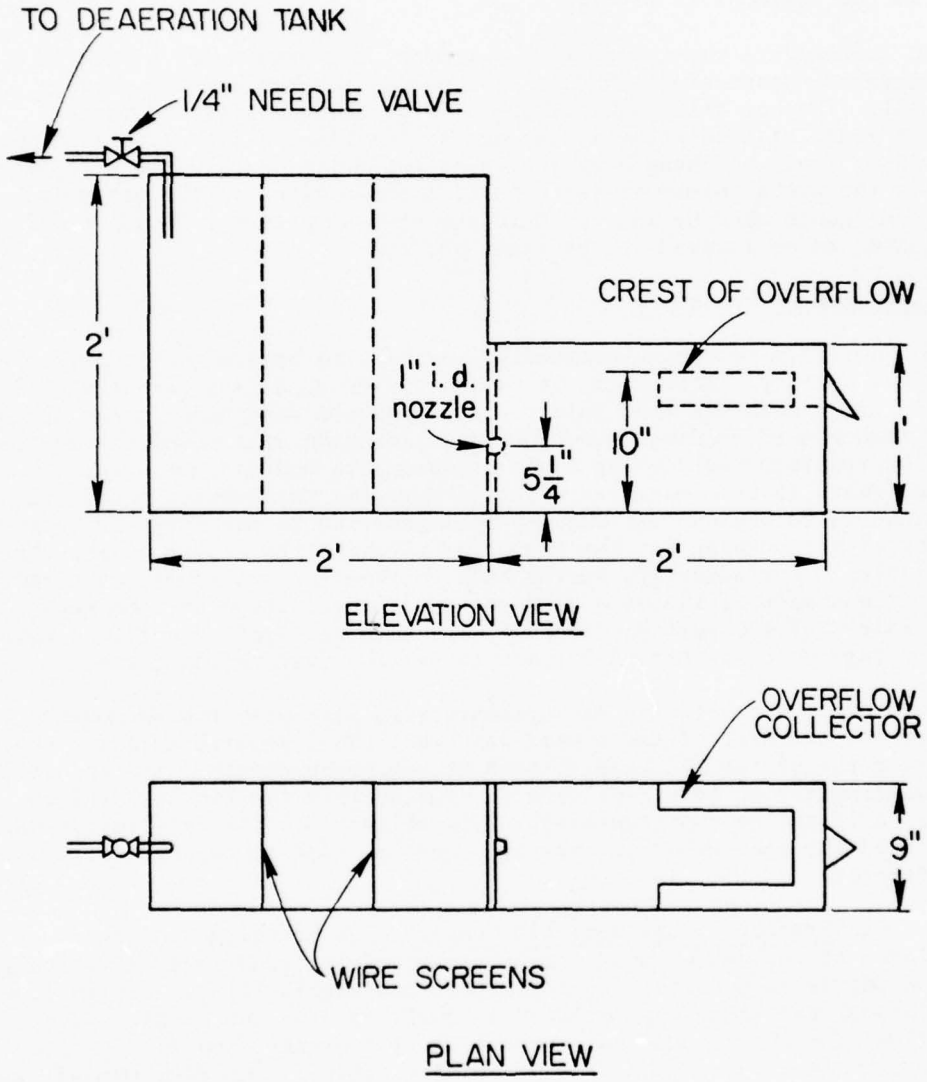

Figure 18. Hot-film anemometer calibration tank.

concentration measurements. To ensure that the natural sediment glued to the artificial dunes did not break loose and damage the sensor, the surface of the dunes was sprayed with a thin film of plastic. The plastic was thin enough to not alter the surface roughness and strong enough to hold the sediment in place.

To accommodate the anemometer equipment, the yoke support used in concentration measurements had to be removed from the support frame (Fig. 3). The hot-film probe assembly (Fig. 19) was attached to the support frame at a position midway across the flume. The elevation of the sensor could be changed by loosening two friction clamps and repositioning the probe holder in relation to a scale fixed to the assembly. A 6-inch-square opening was cut into the wave suppressent board to allow the sensor to be lowered to the flume bottom.

2. Experimental Procedure.

The hot-film sensor is extremely sensitive to both water temperature and water quality. Therefore, it was necessary to determine a new calibration curve each day that velocity measurements were made in the flume. Water temperature readings made during calibration measurements were compared to readings made during flume measurements and did not vary. It was necessary to use deaerated water in both the calibration and flume measurements to prevent air bubbles from adhering to the hot-film sensor, thereby either burning out the sensor or altering its heat transfer characteristics. Periodically, during both calibration and flume measurements a record was made of the base voltage; i.e., the voltage for the sensor in still water. These voltage readings were then averaged to obtain a mean base voltage which is needed in calculating the calibration curve.

Both days that velocity measurements were made with the anemometer, a 5-percent overheat of the sensor was used. This ensured uniform sensitivity of the sensor and base voltage of the measurements. The conditions for measurements on both days were so similar that the two calibration curves could not be distinguished. This allowed all the calibration data to be used for one curve and only one equation used to convert voltage into velocity.

a. Calibration of the Hot-Film Sensor. The hot-film sensor was positioned at the center and as close to the downstream face of the calibration nozzle as possible (approximately one-eighth inch). A high flow rate through the flume was obtained by fully opening the needle valve. This flow rate was allowed to continue until a steady flow through the calibration tank was established (about 5 minutes). The flow through the nozzle was monitored by the continuous voltage output of the hot-film bridge displayed on the anemometer equipment. When the voltage readings became constant with time the flow rate was steady. A 24-second magnetic tape record was then made at the rate of 117 samples per second. Simultaneous with the voltage record, a flow rate measurement was made. The flow rate was determined by timing the period required to collect 10 to

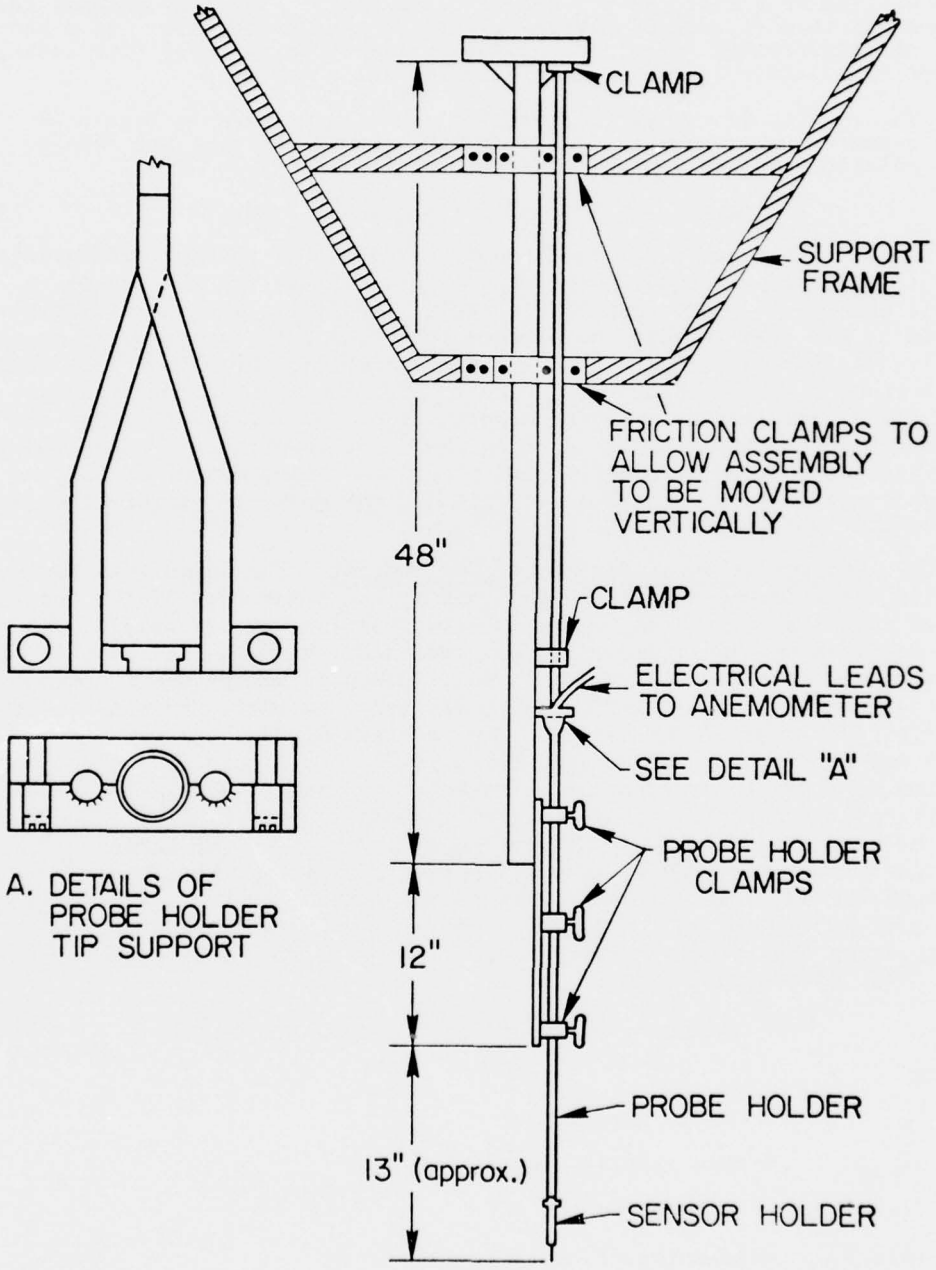

Figure 19. Hot-film probe extension assembly.

15 pounds of water at the overflow of the calibration tank. The water was weighed on a scale to the nearest 0.05 pound. The flow through the flume was then reduced by partially closing the needle valve and a second set of measurements made. The procedure was repeated until five voltage-velocity points were measured for a calibration curve.

The results of the two calibration curves are shown in Figure 20. The velocity range measured was from 0.0374 to 0.580 foot per second. The relationship between velocity and voltage was:

$$\ln_e(E' - E_o) = (0.422)\ \ln_e(U_e) + 7.147\ , \qquad (14)$$

where E' is proportional to the output voltage of the hot-film bridge, and E_o is proportional to the mean output voltage for the sensor in still water. U_e, the actual velocity of the fluid, was calculated by dividing the mean velocity determined from flow rate measurements by the nozzle coefficient, C_n. The log-log relationship shown in Figure 20 is consistent with the theoretical results from the manufacturer and the results by Das (1968). Because magnitudes of the voltage readings for a given flow velocity are dependent on the water temperature, water quality, overheat percentage, and amplification of the sensor output signal, no attempt was made to compare quantitatively the measured calibration curve with other published curves.

b. Determination of the Nozzle Coefficient. The sensor was positioned close to the downstream face and at the lower edge of the nozzle. After establishing a high, constant flow rate through the nozzle, the voltage from the hot-film bridge was recorded. Without interrupting the flow, the sensor was then raised a small measured amount and a second voltage record made. This procedure was repeated until the sensor was at the upper edge of the nozzle. The velocity of flow was estimated for each location from a calibration curve similar to Figure 20 but not corrected by a nozzle coefficient. The velocity profile across the diameter of the nozzle for the high flow rate is shown in Figure 21(a). Because of the high flow rate, the water surface elevation in the deaeration tank was lowering a significant amount, thereby decreasing the flow rate through the calibration tank. This is the reason for the lower measured velocity at the top of the nozzle. The mean velocity was determined by integrating the velocity profile across the jet. The nozzle coefficient was then calculated from:

$$C_n = [(V_{mean})\ (\text{dia.})^2_{jet}]/[(\text{dia.})^2_{noz.}\ (V_{meas.})]\ , \qquad (15)$$

where

C_n = nozzle coefficient

V_{mean} = mean velocity across the jet

$(\text{dia.})_{jet}$ = diameter of the jet

$(\text{dia.})_{noz.}$ = diameter of the nozzle (1 inch)

$(V_{meas.})$ = velocity determined from voltage measurements

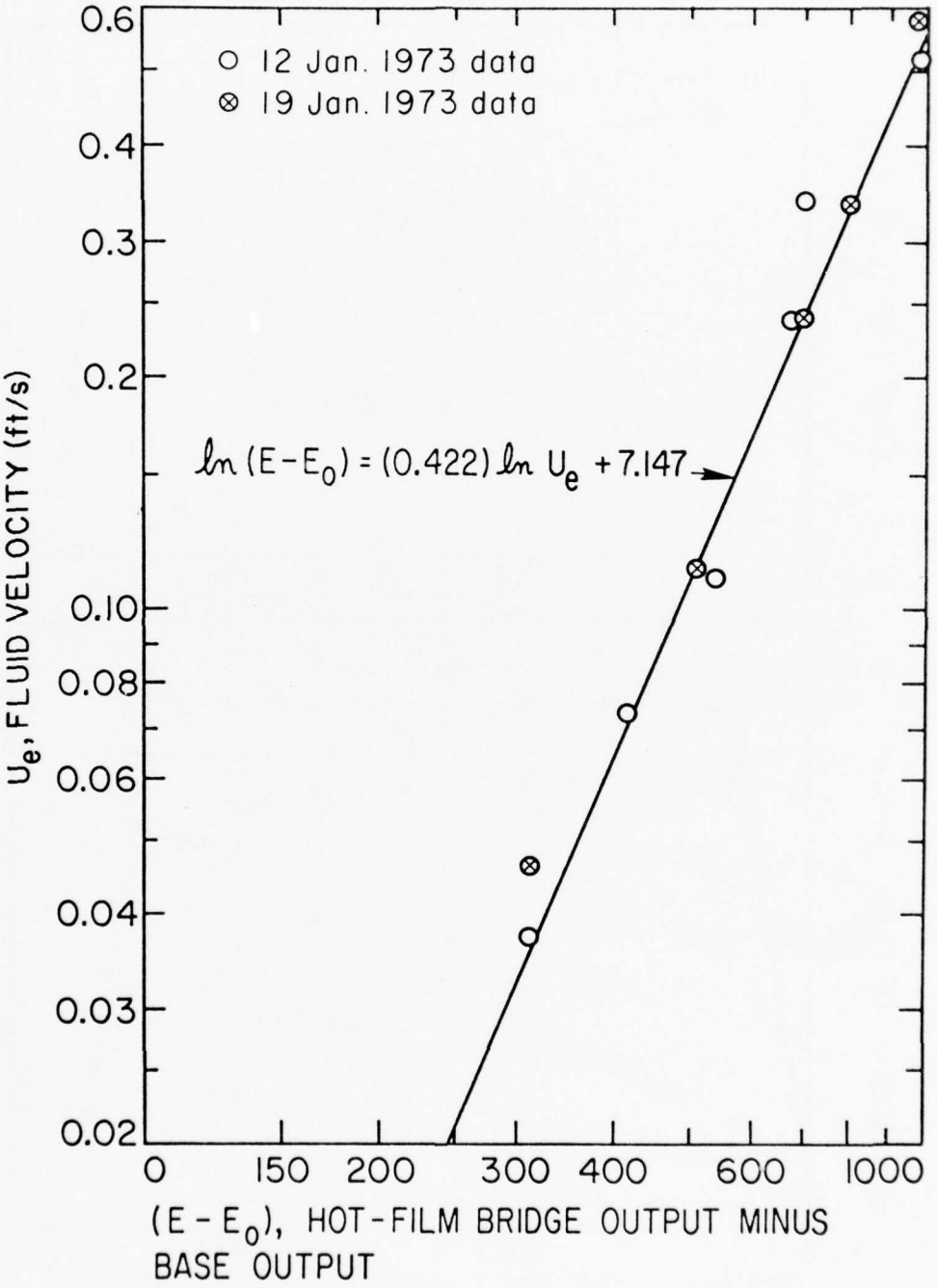

Figure 20. Output versus velocity calibration curve for hot-film anemometer measurements.

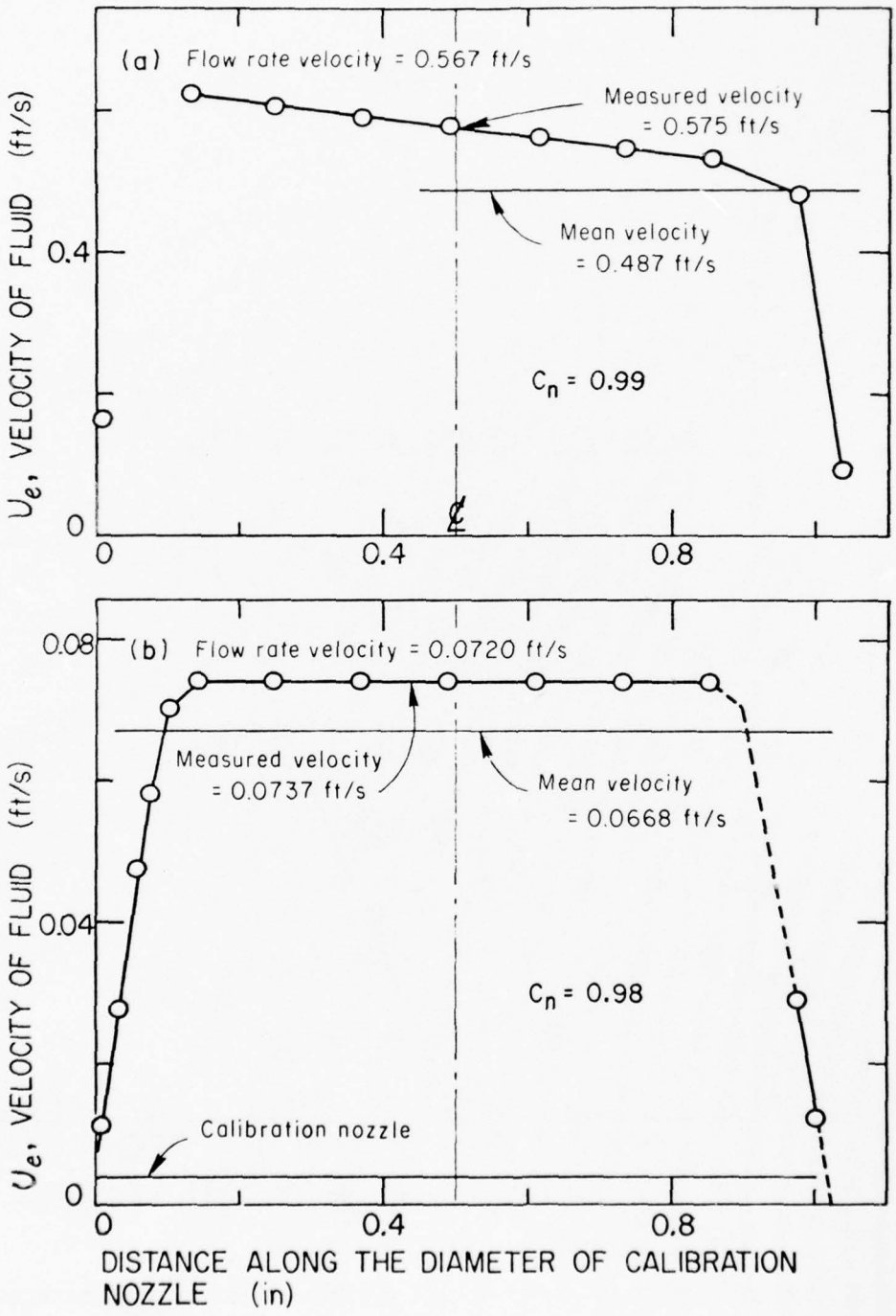

Figure 21. Velocity profile across calibration nozzle.

The nozzle coefficient for the high velocity (0.569 foot per second) was then calculated to be 0.99. This set of measurements was repeated for a low flow rate. The results of these measurements are shown in Figure 21(b). The nozzle coefficient for the low velocity (0.072 foot per second) was calculated to be 0.98. The nozzle coefficient for intermediate velocities was assumed to be a linear interpolation between the two above values.

c. Flume Measurements of Turbulent Velocity Distributions. The velocity, which is of significance in attempting to describe the suspension of sediment in an oscillating flow, is the vertical component of velocity fluctuations due to turbulence, v'. When the swing flume is operating, the only velocities which exist in the fluid are: (a) the three directional components of velocity fluctuations caused by turbulence, and (b) the oscillating flow contained in the boundary layer. The boundary layer extends only a few millimeters above the bed of the flume. Sediment is in suspension at an elevation considerably above the upper limit of the boundary layer. Therefore, the flow regime of interest has no measurable mean or periodic velocities, only the random motions caused by the turbulence diffusing upward from the bed. The problem, then, is to determine only the vertical component of the velocity fluctuations.

Das (1968) developed a method of measuring v' in a still body of water with an oscillating rough bed. This method involved imparting an oscillating motion to the sensor in the vertical direction. If only measurements made during the peak velocity of the sensor are considered, then the total velocity affecting heat transfer from the sensor is:

$$V_e^2 = (V + v')^2 + u'^2 + w'^2 , \qquad (16)$$

where

V_e = total velocity affecting heat transfer

V = peak velocity of the sensor; known from the period and amplitude of oscillation

v' = vertical component of the turbulent velocity fluctuations

u' and w' = turbulent velocity fluctuations in the remaining two directions

Dividing this equation by V^2 yields:

$$(V_e^2/V^2) = 1 + (2\,v'/V) + (v'/V)^2 + (u'/V)^2 + (w'/V)^2 . \qquad (17)$$

If the sensor oscillation is such that $V >> v'$, u', and w', then the above equation can be approximated by:

$$(V_e^2/V^2) = 1 + (2\,v'/V) . \qquad (18)$$

This equation is sensitive to only v'. Experiments by Das were conducted in a stationary flume in which only a horizontal bottom plate was oscillated to produce turbulence. The results showed some promise for the method.

When Das' method of measuring v' was tried in the swing flume, it was not successful because of excessive vibrations of the sensor. These vibrations were mainly due to: (a) the long holder required to extend the sensor to the flume bottom, and (b) attaching this holder to the support frame which was indirectly subjected to the vibrations from the flume motion. The velocities of the sensor due to vibrations were greater than the velocities of the turbulent flow; therefore, no component of turbulent velocity could be distinguished.

An approximation to v' had to be obtained based on the following assumptions. It was assumed that at a given elevation the root-mean-square value of the three components of turbulent velocity fluctuations is proportional to each other. It was also assumed that the heat convected from the sensor due to velocities in the direction parallel to the sensor axis was insignificant compared to the heat convected by velocities perpendicular to the axis. This assumption is justified in that the hot-film has directional properties making the maximum sensitivity at right angles to the flow. Also, the aspect ratio (length-diameter) of the sensor is such that its properties approach those of an infinite wire where there is no effect of a longitudinal velocity. Based on these assumptions, the effective velocity causing heat convection is, as an average:

$$U_e = [v'^2 \ (K'^2 + 1)]^{\frac{1}{2}} , \qquad (19)$$

where U_e is the velocity corresponding to the output voltage of the hot-film bridge, K' is the constant of proportionality between the vertical component and one of the horizontal components of turbulent velocity fluctuation, and v' is the vertical component of the turbulent velocity causing heat convection from the sensor. It is apparent then that the sensor must be placed in the flume with its axis horizontal. The magnitude of the vertical component of velocity fluctuation can then be calculated and is, as an average:

$$v' = [U_e^2/(K'^2 + 1)]^{\frac{1}{2}} . \qquad (20)$$

Although equation (20) is only an approximation, the assumptions used do not affect the basic relationships (a) between the root-mean-square

value of v' and elevation above the bed, and (b) between the root-mean-square value of v' at a fixed elevation and the flow velocity, U_o. The assumptions also allow an approximation of the absolute magnitude of the root-mean-square value of v'. The horizontal component of turbulent velocity fluctuation is probably on the same order of magnitude as the vertical component and therefore, for qualitative analysis, the value of K' in equation (20) can be approximated as equal to unity.

The procedures used in measuring velocity distributions in the flume were as follows. A period and an amplitude of flume oscillation were selected and the flume linkage adjusted to give a symmetric motion. After the flume was filled with deaerated water to the elevation of the wave suppressent board, the asymmetric roughness elements were adjusted to eliminate secondary currents in the central part of the flume. The sensor was then placed in the flume as near the bottom as possible and its elevation recorded. The flume was started and the motion allowed to continue until equilibrium flow conditions were established. A record of the hot-film bridge output voltage was made on magnetic tape, the length of which was an integer multiple of the flume oscillation period. The flume was stopped and the sensor elevation raised for a new measurement. The procedure was repeated until an elevation was reached at which the velocity fluctuations were too small to be accurately measured with the anemometer. The sensor was then lowered in a stepwise manner to obtain velocity measurements at intermediate elevations. In this manner, 10 to 13 velocity-elevation measurements were obtained to give a velocity distribution for the flow condition used. The period of the flume was changed and the measurements repeated to give a second velocity distribution. In all, four velocity distributions were obtained for four different flow conditions.

3. Results.

The purpose of the velocity measurements was to obtain the following three relationships needed for an analysis of the suspended-load equation: (a) An approximation of the magnitude of the root-mean-square value of v' versus flow velocity, U_o; (b) the distribution of the root-mean-square value of v' versus elevation above the bed; and (c) the distribution with time of v' at a constant location in space. Results pertaining to the third unknown listed above will be discussed first.

Two sets of data were analyzed to determine the distribution with time of v'. The period and amplitude of flume oscillation for both sets of data were 10.48 seconds and 0.925 foot, respectively. In both cases, the length of record analyzed was 10.48 seconds (1,224-voltage samples). One set of data was taken at an elevation of 0.168 foot above the crest of the artificial dunes, the other 0.209 foot above.

The data were analyzed in the following manner. For each voltage sample recorded, the effective heat transfer velocity, U_e, was calculated from equation (14). The velocities were ordered and percentages

equal to or less than various selected velocities calculated. These percentages were divided by two and plotted against velocity on normal probability paper. The percentages were divided by two in order to adjust for the fact that the anemometer measured the absolute effective velocity without regard to its direction; i.e., the velocities in each range were composed of an equal number of negative and positive velocities, thereby giving twice the percentage of actual positive velocities. As shown in Figure 22(a, b), these plots approximate straight lines and the 50-percent velocity is zero, thereby indicating that the distribution of the turbulent velocity fluctuations is approximately normal with a mean of zero. Similar data by Das (1968) give the same results.

The above result suggests that the standard deviation, s, of the normal distribution (which equals the root-mean-square velocity) be used as the velocity scale describing turbulence intensity for a given elevation.

The data were then analyzed to determine the distribution of s with respect to elevation. For each sample of a voltage record, the effective heat transfer velocity was calculated from equation (14). From the velocity record, the root-mean-square effective velocity was calculated. Knowing this velocity the velocity scale for the elevation at which the record was made was calculated from:

$$s = \overline{U_e}/\sqrt{2} \ , \tag{21}$$

where s is the velocity scale and is equal to the standard deviation of v' for the elevation of the record and flow conditions of the flume, $\overline{U_e}$ is the root-mean-square effective heat transfer velocity of the record, and $\sqrt{2}$ comes from equation (20) when K' is assumed equal to unity.

The velocity scale was plotted against elevation on semilogarithmic paper to give the relationships shown in Figures 23 to 26. In general, these relationships can be expressed by:

$$s = s_o \exp(A\,Y) \ , \tag{22}$$

where s_o is the value of the velocity scale (in feet per second) at the elevation of the crest of the artificial bed dunes, A is the slope of the exponential curve (in $feet^{-1}$), and Y is the elevation (in feet) above the crest of the bed dunes. The flume flow conditions for which a velocity scale-elevation distribution was measured were U_o = 0.353, 0.510, 0.748, and 0.930 foot per second.

Comparison of the four velocity-elevation distributions revealed that, for the range of flow conditions studied and bed roughness used, the slope of the exponential relationship was constant. This implies that the intensity of the turbulence decreases in a manner which is independent of the flow velocity generating the turbulence. The constant rate of velocity decay appears to apply to elevations near the bed, within 1.5 centimeters as measured with the hot-film sensor.

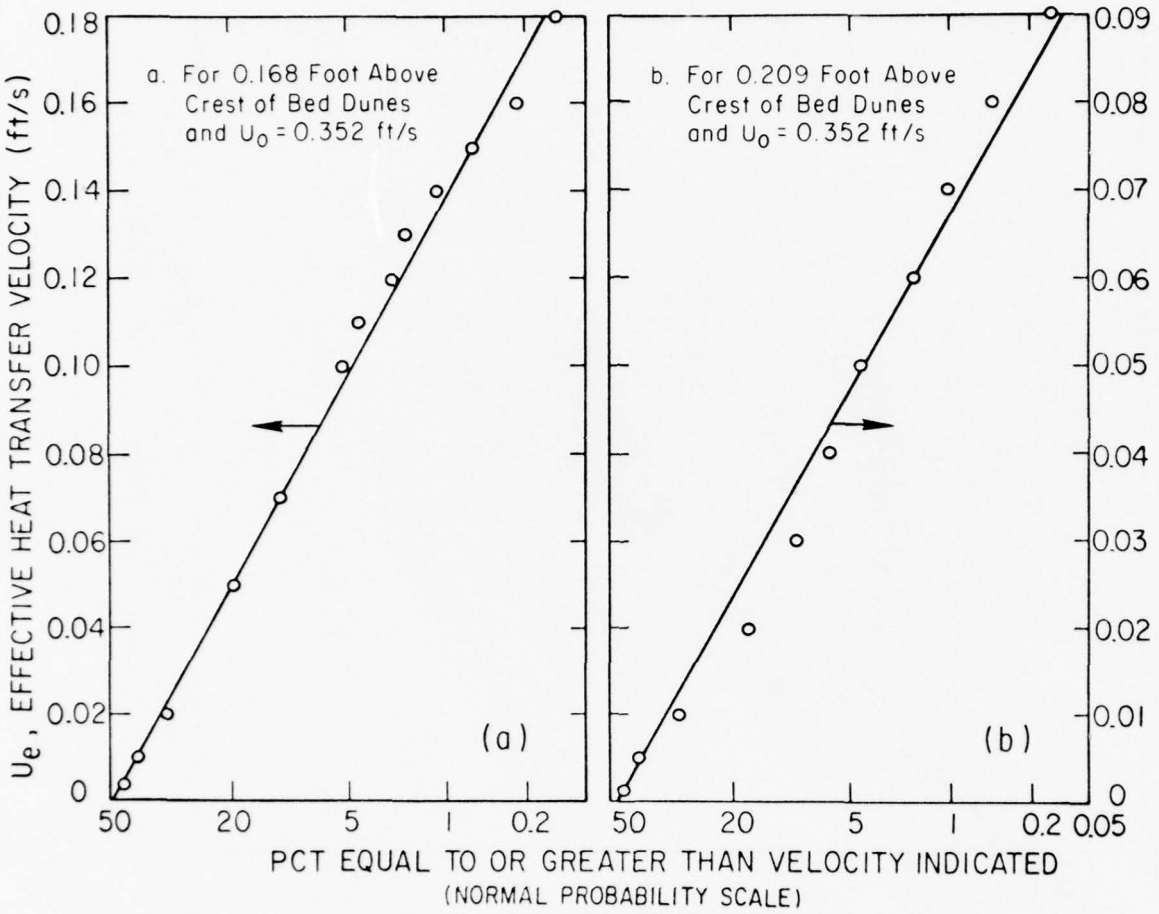

Figure 22. Distribution of turbulent velocity fluctuations.

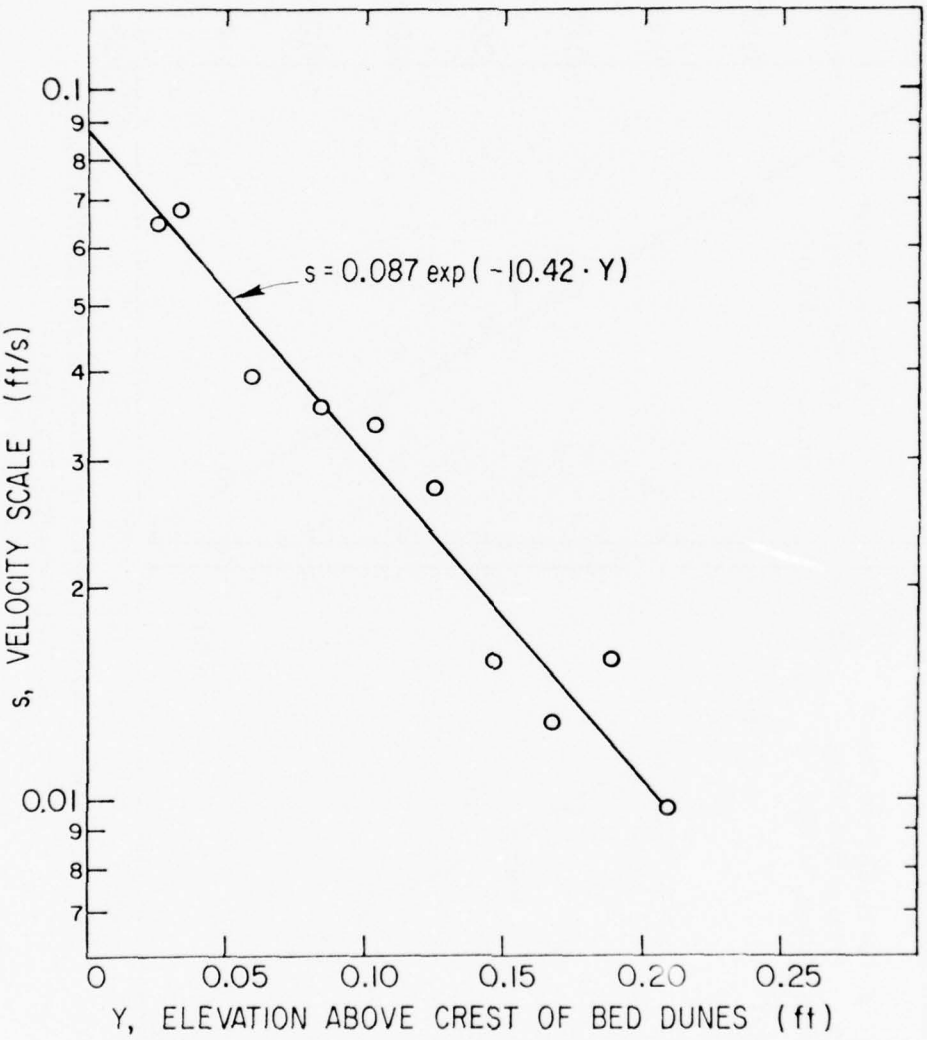

Figure 23. Velocity scale versus elevation for flume velocity, U_o = 0.353 foot per second.

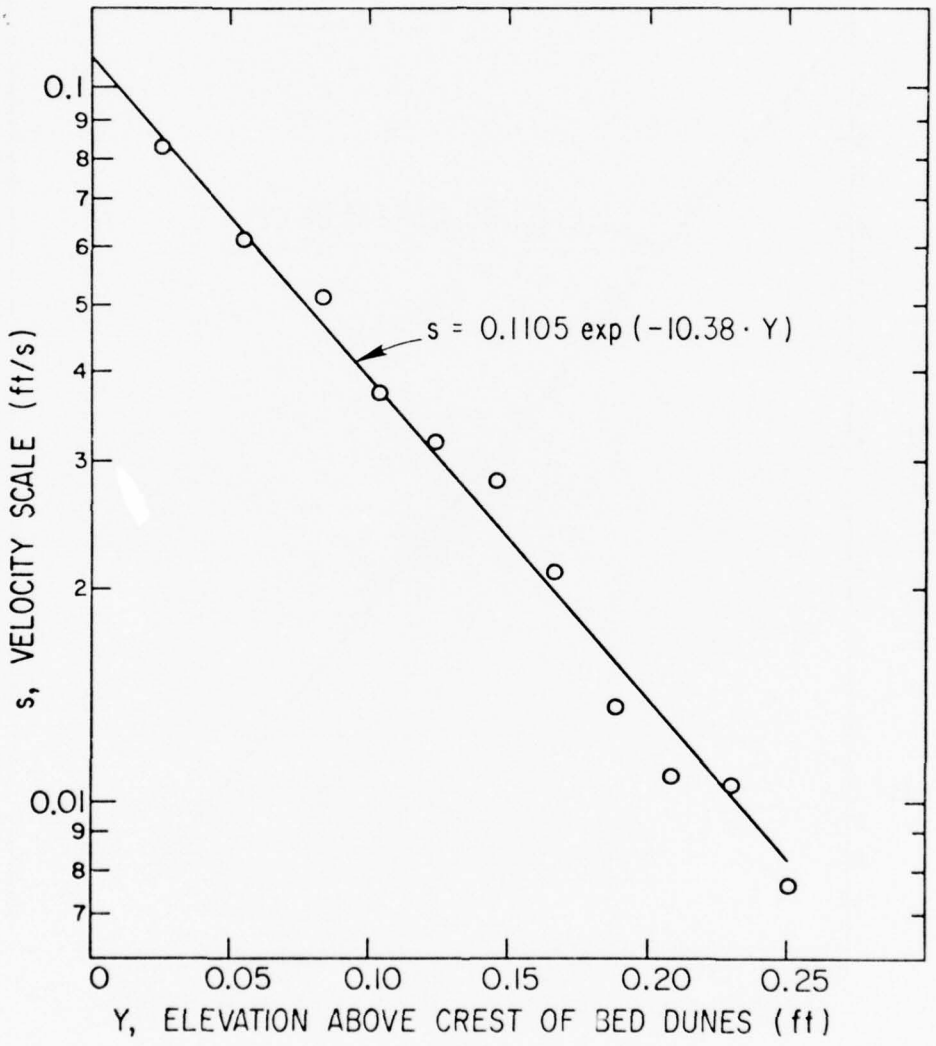

Figure 24. Velocity scale versus elevation for flume velocity, U_o = 0.510 foot per second.

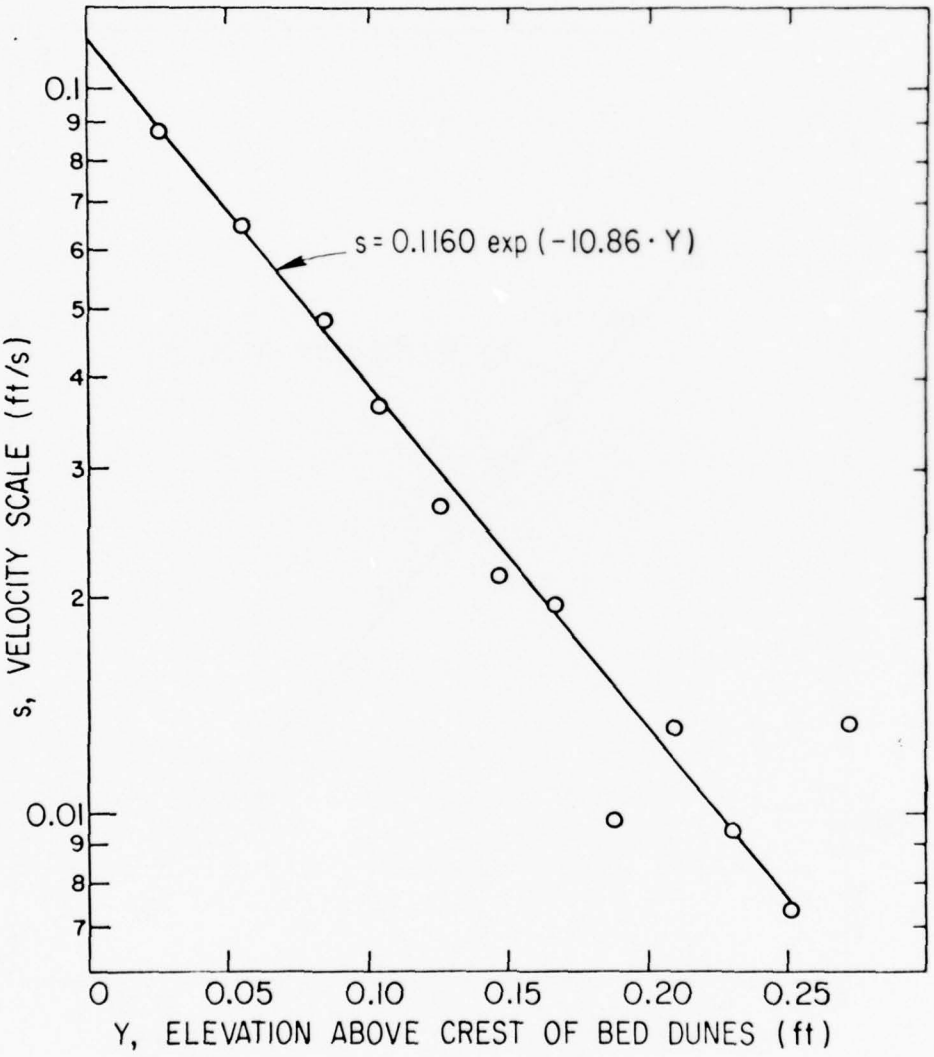

Figure 25. Velocity scale versus elevation for flume velocity, U_o = 0.748 foot per second.

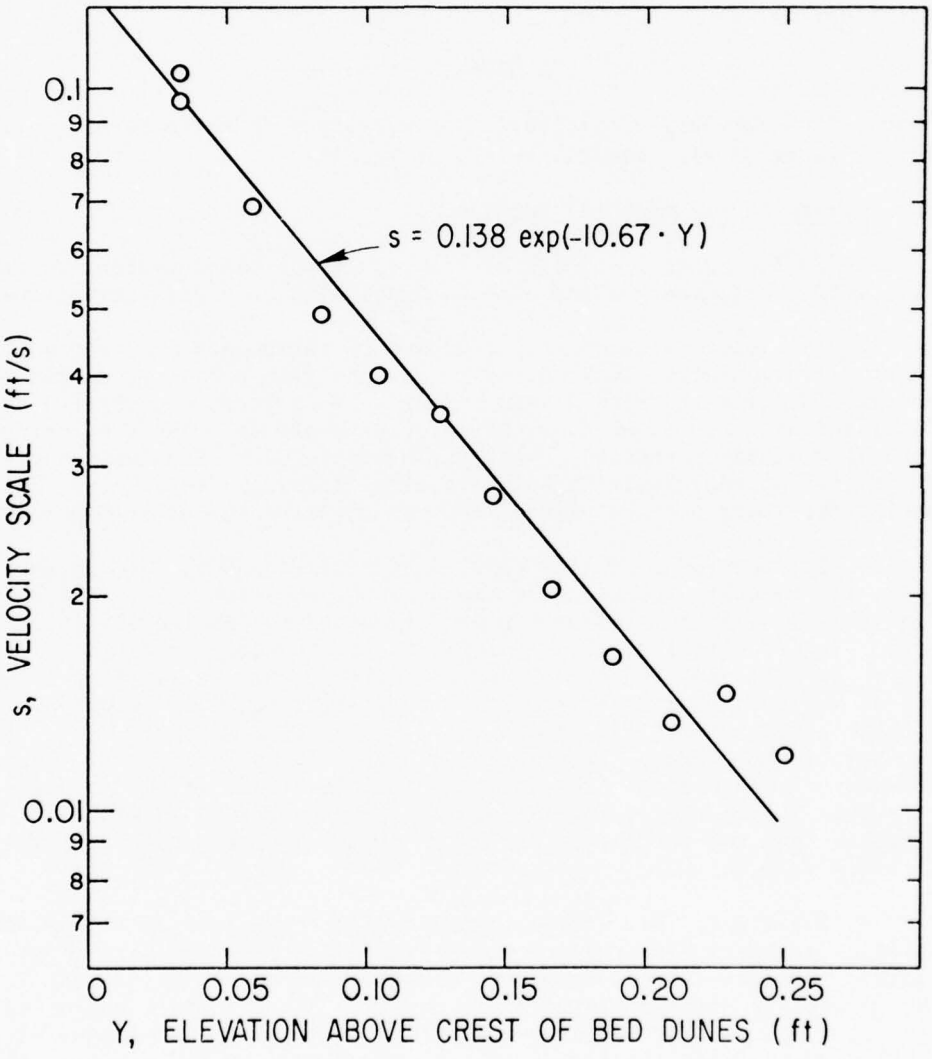

Figure 26. Velocity scale versus elevation for flume velocity, U_o = 0.930 foot per second.

The base velocity, s_o (eq. 22), was found to be a function of the flume flow conditions. The relationship between s_o and U_o is shown in Figure 27. From the limited data it was only possible to determine an approximate mathematical relationship between s_o and U_o. This relationship is:

$$s_o = (0.0885)\ U_o + 0.0557\ , \qquad (23)$$

which, from boundary considerations, only gives approximate s_o values in the range of experimental values of U_o.

4. Summary of Experimental Results.

The following is a summary of the results of the turbulent velocity fluctuation measurements and a brief discussion of their limitations.

a. The velocity fluctuations caused by turbulence are, for a constant elevation above the bed and a constant flow velocity, approximately normally distributed with a mean of zero. The standard deviation of the distribution, s, is used as the velocity scale to measure turbulence intensity at any elevation. Most turbulent velocity fluctuation measurements give approximately Gaussian results, although it is known that except for isotropic turbulence, the distribution cannot be Gaussian.

b. For the range of flow conditions studied and the bed roughness used, the velocity scale can be expressed by equation (22). The exponential nature of this relationship was discussed in Section II, paragraph 4(a). The relationship also conforms to the boundary conditions of the flow. As expected, the turbulence intensity assumes a limiting value, s_o, at the ocean bottom ($Y = 0$). This limiting value of turbulence intensity is determined, in some manner, by the flow velocity, U_o. As the turbulence diffuses upward its intensity decays because of viscosity. The body of fluid into which the turbulence diffuses is, by comparison, extremely large; therefore, the empirical relationship is expected to indicate that the turbulence intensity decays to zero at an infinite distance from the bed.

c. The slope, A, of the exponential distribution of the velocity scale is constant with respect to elevation and constant throughout the range of flow conditions studied. It was found to be -10.57 feet^{-1}. This result is not surprising since the rate of turbulence intensity decay for the oscillating flow conditions measured is determined by viscosity. Therefore, for fluids of the same viscosity and density, the rate of decay should be constant and independent of flow velocity.

d. The base velocity scale, s_o (eq. 22), is a function of the flow velocity and can be approximated by equation (23). This equation is a best fit relationship of the empirical data and does not apply for flow velocities outside the measured range. This becomes obvious by letting $U_o = 0$ foot per second and finding $s_o = 0.0557$ foot per second.

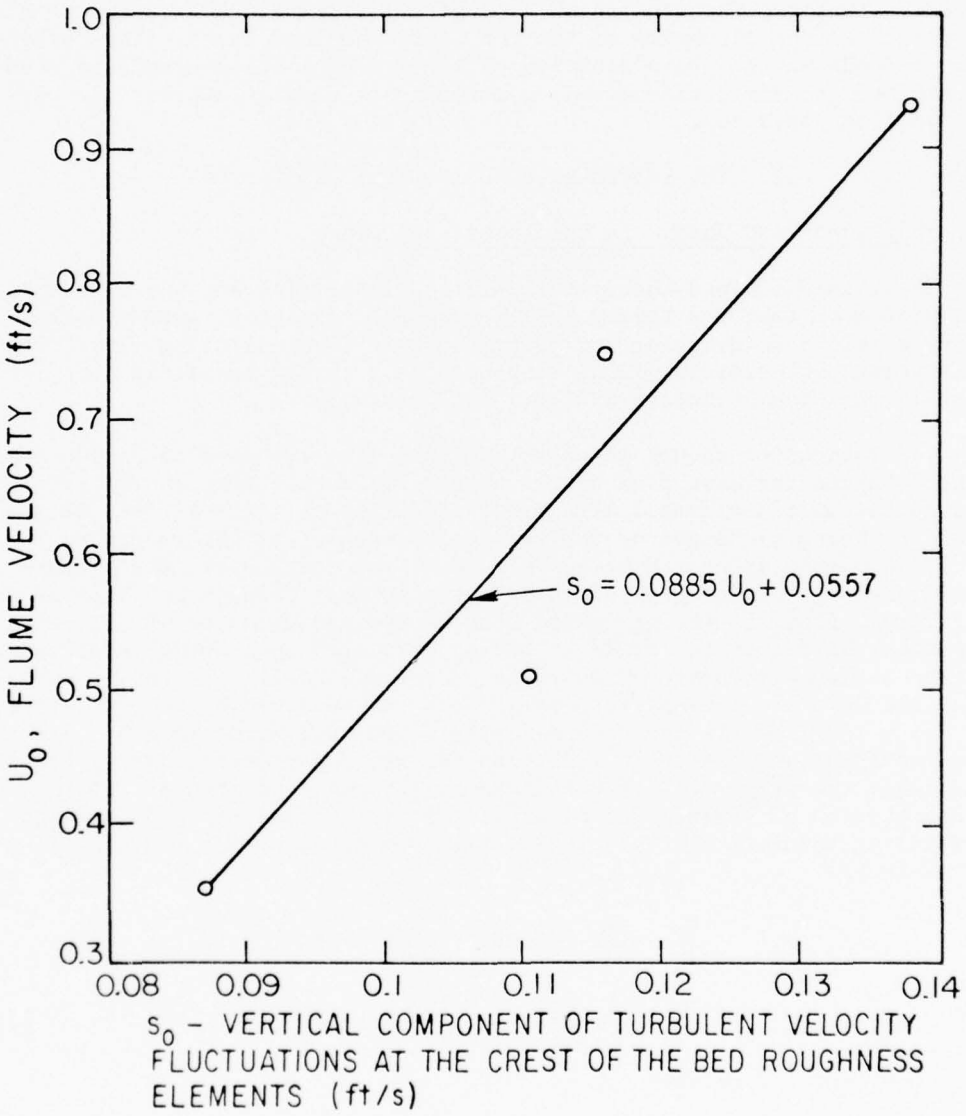

Figure 27. Base vertical turbulent velocity scale versus flume velocity for a constant amplitude = 0.925 foot.

In the range of flow velocities where equation (23) is valid, the calculated s_o is an approximation of a base velocity at an arbitrary elevation, the crest of the bed dunes. To apply the experimental results to a real situation, the constants in equation (23) must be adjusted to give s_o values at the elevation of the top of the bedload layer. This elevation depends on the grain diameter of the sediment being considered and on the bed geometry; therefore, no attempt was made to express s_o at the bedload elevation.

IV. THE SUSPENDED LOAD IN OSCILLATING FLOW

1. Suspended-Load Theory in Unidirectional Flow.

The suspended-load theory for unidirectional flow and the available field data to test the theory supply valuable insight to some problems which exist in determining the suspended load in oscillating flow. For this reason, Einstein's (1950) suspended-load theory and field data from the Missouri and Atchafalaya Rivers are presented.

The suspension theory in unidirectional flow is based on an equilibrium equation for mass flux across a unit horizontal area in the flow. Assume the unit horizontal area is at elevation Y. Across this area fluid is being exchanged by the vertical component of the random motion of fluid particles caused by turbulence. From continuity, the picture of fluid exchange can be simplified by assuming that through one-half of the unit area, fluid is moving upward with an average velocity of v; through the other half area the fluid is moving down with an average velocity -v. If the exchange occurs over an average distance of l_e it can be assumed that the downward-moving fluid originates, as an average, from an elevation Y + 1/2 l_e while the upward-moving fluid originates from Y - 1/2 l_e. The important assumption is made that the fluid preserves, during its exchange, the properties of the fluid at its point of origin. If the concentration of sediment at elevation Y is C and the sediment has a settling velocity of V_s, the equilibrium equation for sediment flux is given by:

$$\left[C - \frac{1}{2} l_e \, (dC/dY)\right] \left(\frac{1}{2}\right) (v - V_s) +$$

$$\left[C + \frac{1}{2} l_e \, (dC/dY)\right] \left(\frac{1}{2}\right) (-v - V_s) = 0 \, . \qquad (24)$$

This equation reduces to:

$$C \, V_s + \frac{1}{2} l_e \, v \, (dC/dY) = 0 \, . \qquad (25)$$

To solve this equation the term, 1/2 l_e v, must be evaluated. This is normally done by equating this term to the corresponding term in a similar equation of momentum exchange; i.e., the sediment exchange coefficient is

assumed equal to the momentum exchange coefficient. Assuming that shear due to viscosity may be neglected, compared with that due to momentum transport, the depth, d, may be introduced:

$$\tau = \tau_o \left[(d-Y)/d\right] = \frac{1}{2} v \rho \left\{\left[u - \frac{1}{2} l_e \left(du/dY\right)\right] - \left[u + \frac{1}{2} l_e \left(du/dY\right)\right]\right\} , \quad (26)$$

where

τ_o = shear stress at the bed; equal to $g\rho RS$

τ = shear stress at elevation, Y

R = hydraulic radius (in feet)

S = energy slope

g = acceleration due to gravity

ρ = density of the water

u = horizontal flow velocity

Using the logarithmic formula based on von Karman's (1934) similarity law for the distribution of flow velocity, du/dY may be calculated:

$$du/dY = (1.0/0.4) \left(u_*/Y\right) , \quad (27)$$

where u_* is the shear velocity and equal to $(\tau_o/\rho)^{\frac{1}{2}}$. Substituting this value into equation (26) and solving for $1/2\ l_e\ v$ yield:

$$\frac{1}{2} l_e\ v = (-0.4)\ Y\ u_*\ (d-Y)/d . \quad (28)$$

Using this value in equation (25), separating variables and introducing the abbreviation:

$$Z = V_s/(0.4\ u_*) , \quad (29)$$

the result can be integrated from a to Y. The solution is:

$$(C/C_a) = \left[(d-Y)\ a/Y\ (d-a)\right]^Z . \quad (30)$$

It has been found that equation (30) gives the correct form of the distribution function, but the value of the exponent Z given by equation (29) does not always agree with the exponent that fits the measured data. Let Z' be the exponent which best fits the data. It was found that for high values of Z (Z>1.0), Z' was significantly less. As Z is

reduced, the difference between Z and Z' decreased and finally when Z assumed values less than unity, which is normally the case, the difference between Z and Z' was small enough such that use of equation (29) allows accurate results. The relationship between Z and Z' is shown in Figure 28 (Einstein and Chien, 1954).

2. Similarities Between Oscillating and Unidirectional Flow.

The similarities between oscillating flow and unidirectional flow with low shear velocities are pronounced. It was found that the concentration distribution in oscillating flow (from equation 9) could be expressed by:

$$C/C_o = \exp(M\,Y) \ , \tag{31}$$

where M was found in Section II to be (from equation 13):

$$M = -V_s/E \ , \tag{32}$$

E is the sediment exchange coefficient. The coefficient, M, which defines the rate at which the concentration decays with elevation, behaves in a manner similar to Z of the unidirectional flow theory. In oscillating flow, as in unidirectional flow, the value of M fitting the experimental results was different than the value which would be predicted from equation (32), assuming E independent of V_s. Figure 15 and Table 3 show that for the four concentration distribution curves obtained when V_s was increased from 0.035 to 0.0626 foot per second, the absolute value of M increased, as an average, by the factor 1.19. When V_s was increased from 0.035 to 0.0498 foot per second, the absolute value of M increased, as an average, by 1.13. If the exchange coefficient, E, of equation (32) were a function of the flow hydraulics only and independent of the sediment-settling velocity, then the average increase in the absolute value of M would have been 0.0626/0.035 (= 1.8) and 0.0498/0.035 (= 1.42), respectively. Therefore, it can be concluded that the sediment exchange coefficient, E, is a function of both V_s and U_o, and that M, for a constant flow velocity, is not directly proportional to V_s. This conclusion agrees with Einstein and Chien (1954) that in unidirectional flow for high values of settling velocity relative to the flow shear velocity the sediment exchange coefficient cannot be accurately approximated by the momentum exchange coefficient.

The difference between the sediment and momentum exchange coefficients depends on the relative magnitudes of the sediment-settling velocity and the turbulence intensity. If the sediment-settling velocity is small compared to the turbulence intensity, the two coefficients are approximately equal; when $V_s = 0$, the two coefficients are identical. As V_s becomes relatively larger, the difference between the two coefficients increases. In unidirectional flow the turbulence intensity is usually very large compared to V_s and the theory is accurate under most situations. Unfortunately, this is usually not the case in oscillating flow.

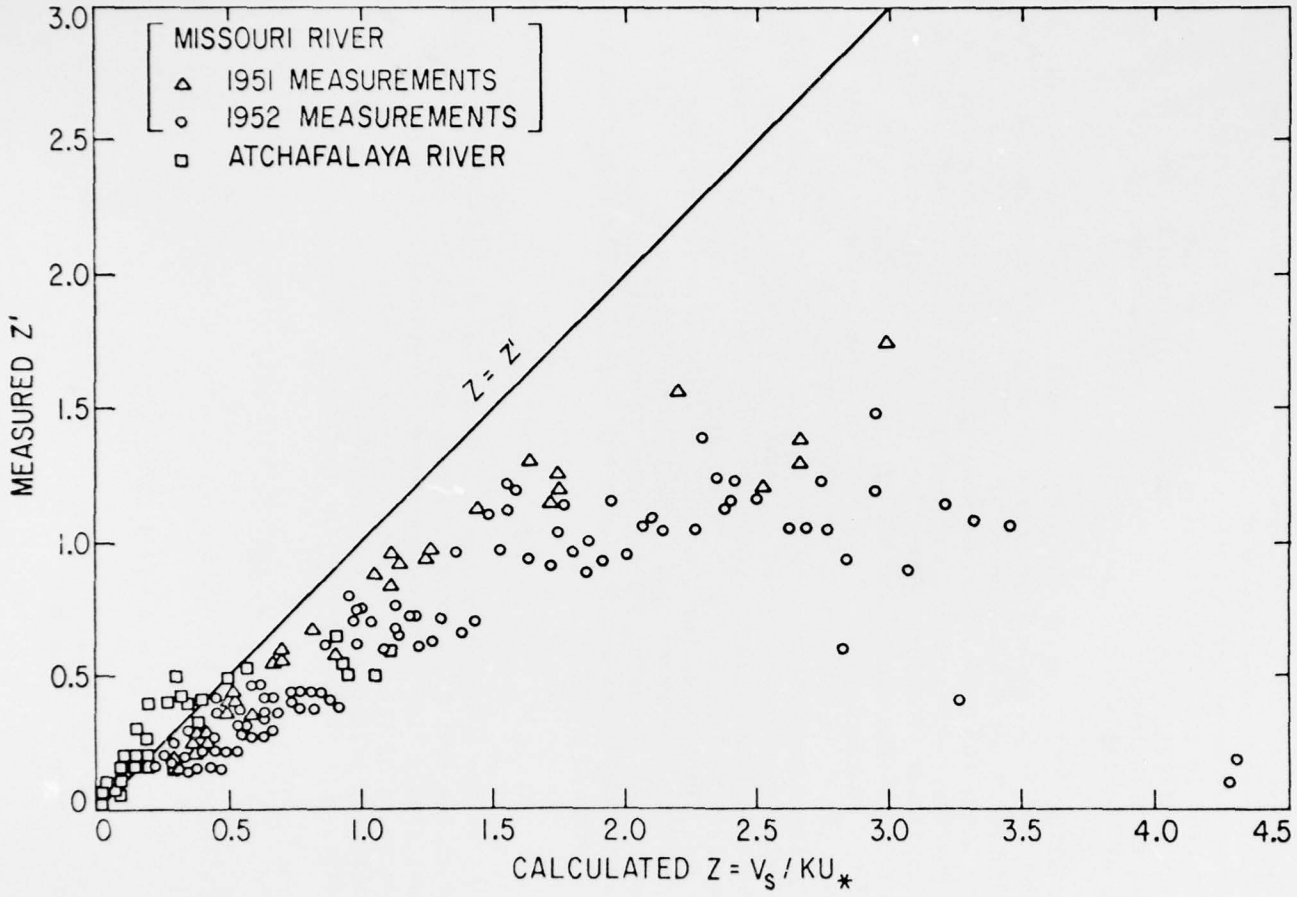

Figure 28. Comparison of the theoretical and measured exponent of concentration distribution in unidirectional flow (from Einstein and Chien, 1954).

Examining results b, c, and d of Section III, the range of the root-mean-square value of v' (s) is $0.0072 < s < 0.103$ foot per second. The settling velocities of the sediments used in the experiments were $V_s = 0.035$, 0.0498, and 0.0626 foot per second. V_s is then, the same order of magnitude as the velocity scale. As discussed earlier, the sediment used in the experiments had a specific gravity of 1.25. Therefore, the settling velocity of natural sediment would be even larger compared to turbulence intensity in the approximate prototype flow conditions of the experiments.

For illustration, a typical oscillatory flow condition of this investigation will be approximated as a quasi-steady unidirectional flow and compared to the field data of Figure 28. This is possible because the time scale for oscillation is much greater than the time scale of the turbulence. For example, the average flow had a period of 6 seconds and an amplitude of about 1 foot, $U_o = 0.667$ foot per second. A time scale of turbulence can be defined as δ/s_o, where δ is the thickness of the boundary layer and s_o is the base vertical velocity fluctuation. If δ is defined as the distance above the bed at which the boundary layer oscillation velocity is equal to 99 percent of the free-stream velocity (velocity given by linear wave theory for $y = -d$), δ can be calculated from equation (5). This calculation indicates that δ is equal to or less than 0.05 foot and from Figure 27, s_o is 0.11 foot per second. Therefore, the time scale for the turbulence is 0.45 second as compared to a 6-second time scale for the oscillation. To calculate the theoretical Z value for the quasi-steady unidirectional flow it is necessary to determine a mean flow shear velocity. The flow shear velocity is given by:

$$u_* = (g\ R\ S)^{\frac{1}{2}} , \tag{33}$$

where R is the hydraulic radius (in feet), g is the acceleration due to gravity (in feet per second squared), and S is the energy slope of the quasi-steady flow. The energy slope is obtained from Manning's equation by using the root-mean-square flow velocity ($= 0.707\ 2\ \pi\ L/T$), and estimating values of the roughness coefficient, n, and the hydraulic radius, R. The expression for the energy slope is:

$$S^{\frac{1}{2}} = (n/R^{0.667})\ (3\ L/T) . \tag{34}$$

Substituting equation (34) into equation (33) yields:

$$u_* = (17\ n\ L)/(T\ R^{0.167}) . \tag{35}$$

Using the above expression for u_* in equation (29), the Z value for the quasi-steady flow becomes:

$$Z = (V_s\ T\ R^{0.167})/(6.8\ n\ L) . \tag{36}$$

For the average flow conditions, V_s is 0.035 foot per second, T is 6 seconds, and L is 1.0 foot. Based on the bottom roughness shape and the hydraulic radius, n is approximately 0.015 foot$^{0.167}$. The hydraulic radius is estimated from the flow geometry as about equal to unity. Since Z is proportional to R to the 0.167 power, and therefore tends to unity, there is probably not much error in using this estimate. Using these values in equation (36) yields Z = 2.1. In Figure 28, this value of Z is well into the range where the sediment exchange coefficient is significantly different from the momentum exchange coefficient.

Because not enough data were obtained to define a relationship between M and V_s and because the sediment exchange coefficient could not be expressed as a function of the shear-stress distribution, no attempt was made to derive a theoretical relationship for the concentration distribution as was done in Einstein and Chien (1954) for unidirectional flow.

3. Sediment Suspension in an Oscillating Flow.

This investigation was done to determine the behavior of sediment suspension in an oscillating flow and present a method by which the suspended load could be approximated from flow hydraulics. It is apparent from the field measurements of unidirectional flow (Fig. 28), and the results of this investigation for oscillating flow that the mechanism by which sediment is held in suspension is complex and not fully understood. For this reason, the following method for estimating the suspended load in oscillating flow as a function of the flow hydraulics is based on the general turbulent mixing length theory first proposed by O'Brien (1933). His derivation is as follows:

There is a continuous up and down motion of fluid across any horizontal plane caused by the turbulent vertical velocity fluctuations. This exchange motion is capable of transporting suspended matter. Consider a horizontal reference section of unit area at a distance Y from the bed. The transfer of sediment in the vertical direction from the region of high concentration to a region of low concentration through this unit section will be $-1/2\ l_e\ v\ dC/dY$, where l_e is the mixing length for the sediment exchange, v denotes the exchange discharge through the unit area due to vertical velocity fluctuations, and C is the concentration of suspended sediment with settling velocity, V_s, at elevation Y. However, a continuous settling of particles through the unit area at a rate of $C\ V_s$ exists. A statistical equilibrium condition is given by equation (25). This equation is identical to the equation derived by Einstein (1950), but without the assumption that the origin of the sediment is the same as the origin of the fluid and without assuming any distribution of fluid exchange.

The mixing length theory incorporates all of the factors which affect sediment suspension in two artificial variables, the velocity scale and the length scale. The velocity scale for oscillating flow was measured

directly in this investigation and is given by equation (22). The sediment exchange coefficient which is the product of the length and velocity scales was also measured directly and is given by equation (13). From these two equations, the corresponding length scale can be calculated as:

$$\frac{1}{2}l_e = (-V_s/M\, s_o)\, \exp(-A\, Y) \qquad (37)$$

For the limited flow conditions investigated, all the variables of equations (13), (22), and (37) have been found as a function of U_o, where U_o is a function of the surface wavelength, period, and water depth. The variable A was found to be a constant (= -10.57 feet^{-1}), and M and s_o are graphically given in Figures 6 and 27, respectively. These expressions for the velocity and length scales are physically reasonable. Not only is the base turbulent velocity a function of the surface wave intensity (Fig. 27), but the exchange length tends to small values as the ocean bed is approached, indicating that no sediment should be exchanged across the bed surface.

4. The Base Concentration, C_o.

With the exception of the base concentration, C_o, all the variables needed to describe the suspended load as a function of flow hydraulics have been discussed. The following is only a brief discussion of the base concentration. Kalkanis (1964) provides a complete mathematical derivation.

In oscillating flow, as in unidirectional flow, sediment transport is by two different types: (a) Bedload transport, and (b) suspended-load transport. As discussed in Section I, the thickness of the bedload layer is about two-grain diameters. Therefore, for both prototype and experimental sediments, the bedload is contained in the boundary layer described in Section II. The theory proposed by Kalkanis to predict the amount of bedload transport and the concentration of sediment is general and only requires knowledge of the surface wave characteristics, the water depth, the bed sediment characteristics, and statistical parameters which have been found experimentally. Because the thickness of the bedload layer is small, the concentration of sediment in this layer is assumed constant and equal to C_o. The concentration, C_o, for the bedload is the base concentration to be used for the suspended load.

Using C_o as the suspended-load concentration incorporates a small error in the total suspended load. As indicated previously, the bedload is contained in the boundary layer. The distribution of sediment concentration in this area is unknown. Because the distance between the top of the boundary layer and the top of the bed layer is small, extension of the exponential suspension distribution down to the bed layer would incur only a minor error in the total amount of sediment in motion.

5. Net Transport of Sediment in the Ocean.

The initiation of sediment movement in the ocean is by wave action. Since the waves are approximately linear, the wave-induced fluid motion is a symmetric oscillation causing an equally symmetric movement of the sediment. This motion ordinarily cannot cause net transport of sediment, but it does suspend sediment so that currents superimposed on the oscillating velocity will cause a net transport of the sediment. Examples of unidirectional currents in the ocean are the longshore current caused by waves attacking the coastline at an acute angle and the secondary currents caused by the coastline geometry. These two examples indicate that determination of the transporting current should be by field measurement.

6. Additional Investigations Needed to Complete the Suspension Theory.

The suspended-load theory is by no means complete. The relationship between the rate of decay of sediment concentration, M, and sediment-settling velocity, V_s, is needed. Figure 15 indicates that settling velocity has a significant affect on the distribution of sediment concentration, but there are not enough data to indicate the relationship. Additional measurements are required to quantitatively determine the relationship between M and V_s for a constant U_o.

Another variable affecting the suspended-load theory and not studied in this investigation is the bed roughness. It is probable that a change in bed roughness would affect the intensity of turbulence at a given elevation. Also, as discussed in Section II, the amplitude of oscillation relative to the wavelength of the bed roughness has an affect on the distribution of suspended sediment. Determination of how the bed roughness affects sediment suspension requires a great deal of experimentation; however, the results of this investigation will supply some guidelines which would reduce the amount of experimental work required.

7. Conclusions.

These experiments in an oscillating flow simulating wave motion at the ocean floor provide results which, in some cases, substantiate previous results and provide new information on the behavior of sediment suspension. It should be stressed that the conclusions of this investigation are confined to the rather limited range of the variables studied.

The conclusions obtained from sediment concentration measurements are:

a. The relationship between the mean sediment concentration and elevation above the bed is exponential. This conclusion is based on 65 concentration distribution relationships covering a wide range of prototype flow conditions and each composed of numerous point concentration measurements. Typical examples of this relationship are shown in Figure 5 and the basic data substantiating this conclusion are given in the appendix. Although this relationship was determined using an artificial

sediment with a settling velocity less than found in the prototype, results of experiments by other investigators using prototype sediments resulted in the same exponential relationship. In addition, the bed roughness used by other investigators varied; therefore, this conclusion does not appear to be limited to the single-bed roughness used in this investigation.

b. Using the above conclusion and the O'Brien's (1933) equation for continuity of sediment exchange results in a sediment exchange coefficient which is independent of elevation above the bed. Behavior of the rate of sediment concentration decay with elevation, which is related to the sediment exchange coefficient by equation (13), was found to be a function of the flow velocity causing the suspension and the settling velocity of the sediment. A linear relationship between the flow velocity and the sediment concentration decay rate was found for the constant sediment-settling velocity used in the majority of the experiments. This relationship is shown in Figure 6. The relationship between flow velocity and the sediment concentration decay rate for other sediments studied in this investigation is shown in Figure 15. The limited data indicate a possible linear relationship for the different sediment-settling velocities. There is not enough data to determine the relationship between the concentration decay rate and settling velocity for a constant flow velocity. Only qualitative conclusions can be obtained from the eight concentration distribution measurements shown in Figure 15. For a constant bed roughness and flow velocity, a higher sediment-settling velocity results in a higher sediment concentration decay rate. The limited data consistently indicate that the concentration decay rate is not proportional to the settling velocity to the first power; i.e., they are not directly proportional. This and equation (13) imply that the settling velocity is an important variable influencing the sediment exchange coefficient. Therefore, in oscillating flows the sediment exchange coefficient cannot be accurately approximated by the momentum exchange coefficient as is commonly done in unidirectional flow analysis. No experiments were conducted in this investigation to determine how the above relationships would change with a change in bed roughness.

The conclusions obtained from measurements of the turbulent velocity fluctuations are:

a. The distribution of turbulent velocity fluctuations at a constant elevation in an oscillating flow was found to be approximately normal with a mean of zero. This relationship was determined from distribution analyses of measurements made at two elevations above the bed, both of which were above the boundary layer described in Section II. Results of these analyses are shown in Figure 22.

b. The relationship between the root-mean-square turbulent velocity fluctuation and elevation above the bed was found to be exponential. This conclusion is based on measurements of distributions made for four different flow velocities, all using an amplitude of oscillation of 0.925 foot and covering approximately the same range of prototype flow velocities as

studied in the concentration measurements. Results of these measurements are shown in Figures 23, 24, 25, and 26, and are tabulated in the appendix, Table A-5. This relationship was valid for elevations of approximately 0.04 foot above the crest of the bed dunes. The relationship below this elevation, which would be in the boundary layer, was not determined. The turbulent velocity fluctuation distribution was only measured for the single-bed roughness described in Section II.

c. Based on the four turbulent velocity fluctuation distributions described above, it was concluded that the rate of turbulent velocity decay with elevation above the bed is independent of both the elevation and the flow velocity generating the turbulence. The exponential decay rate, determined from a least squares curve fitting of the data, for the four distributions ranged from -10.38 to -10.86 $feet^{-1}$, with a mean of -10.57 $feet^{-1}$ and a variance of 0.05 $foot^{-2}$.

d. The relationship between the flow velocity and the root-mean-square turbulent velocity fluctuation at zero elevation (calculated from the empirical relationships) is shown in Figure 27. A linear relationship is indicated. However, this relationship, which is far from conclusive, is based on only four data points with a significant amount of scatter. The qualitative conclusion that the turbulence intensity at zero elevation becomes larger with greater flow velocities is not only indicated by the data but is logical.

LITERATURE CITED

ABOU-SEIDA, M.M., "Bed Load Function Due to Wave Action," Technical Report No. HEL-2-11, Hydraulic Engineering Laboratory, University of California, Berkeley, Calif., 1965.

DAS, M.M., "Extended Application of a Single Hot-Film Probe for the Measurement of Turbulence in a Flow Without Mean Velocity," Technical Report No. HEL-2-20, Hydraulic Engineering Laboratory, University of California, Berkeley, Calif., 1968.

DAS, M.M., "Mechanics of Sediment Suspension Due to Oscillatory Water Waves," Technical Report No. HEL-2-32, Hydraulic Engineering Laboratory, University of California, Berkeley, Calif., 1971.

EINSTEIN, H.A., "The Bed-Load Function for Sediment Transportation in Open Channel Flows," Technical Bulletin No. 1026, U.S. Department of Agriculture, Soil Conservation Service, Washington, D.C., 1950.

EINSTEIN, H.A., and CHIEN, N., "Second Approximation to the Solution of the Suspended Load Theory," M.R.D. Sediment Series No. 3, Institute of Engineering Research, University of California, Berkeley, Calif., 1954.

KALKANIS, G., "Observation of Turbulent Flow Near An Oscillating Wall," M.S. Thesis, University of California, Berkeley, Calif., 1957.

KALKANIS, G., "Transportation of Bed Material Due to Wave Action," TM-2, U.S. Army, Corps of Engineers, Coastal Engineering Research Center, Washington, D.C., Feb. 1964.

KENNEDY, J.F., and LOCHER, F., "Sediment Suspension by Water Waves," *Waves on Beaches*, Academic Press, New York, 1972.

LAMB, H., *Hydrodynamics*, Dover Publications, New York, 1932.

LI, H., "Stability of Oscillatory Laminar Flow Along A Wall," TM-47, U.S. Army, Corps of Engineers, Beach Erosion Board, Washington, D.C., Aug. 1954.

MANOHAR, M., "Mechanics of Bottom Sediment Motion Due to Wave Action," TM-75, U.S. Army, Corps of Engineers, Beach Erosion Board, Washington, D.C., June 1955.

O'BRIEN, M.P., "Review of the Theory of Turbulent Flow and its Relation to Sediment Transportation," *Transactions, American Geophysical Union*, Apr. 1933, pp. 487-491.

SHINOHARA, K., et al., "Sand Transport Along A Model Sandy Beach by Wave Action," *Coastal Engineering in Japan*, Vol. 1, 1958.

VON KARMAN, T., "Turbulence and Skin Friction," *Journal of the Aeronautical Sciences*, Vol. 1, No. 1, Jan. 1934, pp. 1-20.

BIBLIOGRAPHY

BIJKER, E.W., "Littoral Drift Computations on Mutual Wave and Current Influence, Delft University of Technology, Department of Civil Engineering, Delft, The Netherlands, 1971.

EATON, R.O., "Littoral Processes on Sandy Coasts," *Proceedings of the First Conference on Coastal Engineering*, 1950.

EINSTEIN, H.A., "A Basic Description of Sediment Transport on Beaches," *Waves on Beaches*, Academic Press, New York, 1972.

EINSTEIN, H.A., and LI, H., "The Viscous Sublayer Along A Smooth Boundary," *Transactions, American Society of Civil Engineers*, Vol. 123, 1958, pp. 293-317.

HENDERSON, F.M., *Open Channel Flow*, Macmillan, New York, 1971.

JOHNSON, J.W., "Sand Transport by Littoral Currents," *Proceedings of the Fifth Hydraulic Conference*, 1953.

MILNE-THOMSON, L.M., *Theoretical Hydrodynamics*, Macmillan, New York, 1969.

SUTHERLAND, A.J., "Proposed Mechanism for Sediment Entrainment by Turbulent Flows," *Journal of Geophysical Research*, Vol. 72, No. 24, 1967.

WIEGEL, R.L., *Oceanographical Engineering*, Prentice-Hall, Englewood Cliffs, N.J., 1964.

APPENDIX

EXPERIMENTAL DATA

Table A-1. Basic data, concentration distribution measurements, V_g = 0.035 foot per second, amplitude ≥ 0.693 foot.

Curve No. (U_o, ft/s)	Concentration (g/l)	Elevation (cm)
518.01 (1.00)	2.114	2.21
	0.850	7.21
	0.472	12.26
	0.121	17.28
	0.083	19.61
	0.237	14.71
	0.557	9.66
	1.339	4.61
518.02 (0.681)	0.686	4.61
	0.353	7.61
	0.168	10.61
	0.047	13.61
	0.100	12.11
	0.214	9.09
	0.425	6.16
	0.889	3.11
	1.385	1.69
	1.810	0.71
518.03 (0.470)	1.339	0.71
	0.520	2.71
	0.253	4.68
	0.110	6.69
	0.076	8.21
	0.165	5.71
	0.286	3.71
	0.633	1.73
518.04 (0.394)	0.622	1.73
	0.317	3.21
	0.155	4.66
518.05 (0.330)	0.376	0.71
	0.181	2.21
	0.091	3.71
	0.045	5.21
	0.046	4.44
	0.119	2.96
	0.263	1.46
602.01 (1.157)	2.935	2.46
	1.540	7.41
	0.499	12.41
	0.249	17.36
	0.073	19.86
	0.415	14.91
	0.892	9.93
	2.057	4.89
602.02 (0.737)	1.047	4.89
	0.174	8.86
	0.074	10.89
	0.065	11.88
	0.036	12.89
	0.374	6.91
	1.489	3.89
	1.860	2.91
	2.524	1.86
602.03 (0.504)	1.214	1.86
	0.530	3.86
	0.222	5.86
	0.119	7.36
	0.050	9.89
	0.072	8.86
	0.126	6.89
	0.633	2.92
	1.236	0.93
602.04 (0.420)	1.956	0.93
	0.747	2.88
	0.335	4.91
	0.138	6.88
	0.068	8.91
	0.093	7.91
602.05 (0.348)	0.926	1.91
	0.227	3.88
	0.073	5.88
	0.058	7.91
	0.026	8.89
	0.051	6.91
	0.164	4.91
	0.454	2.91
	0.977	0.68
602.06 (0.292)	0.415	2.64
	0.048	6.64
	0.037	7.84
	0.088	5.66
	0.254	3.69
	0.812	1.68
602.07 (0.235)	0.753	0.64
	0.187	2.66
	0.095	4.64
	0.058	5.66
	0.113	3.66
	0.304	1.69
612.01 (0.422)	1.986	1.69
	0.668	3.63
	0.238	5.61
	0.099	7.62
	0.145	6.61
	0.395	4.59
	1.159	2.63
612.02 (0.504)	1.859	2.41
	0.651	4.39
	0.225	6.41
	0.146	8.41
	0.126	9.39
	0.215	7.39
	0.468	5.41
	0.926	3.37
612.03 (0.600)	1.705	3.37
	0.607	5.39
	0.340	7.36
	0.124	10.38
	0.228	8.36
612.04 (0.721)	1.164	4.39
	0.707	6.36
	0.384	8.41
	0.212	10.36
	0.793	5.38
612.05 (1.041)	1.446	5.38
	1.002	8.41
	0.657	11.41
	0.440	14.39
	0.181	17.41
	0.256	15.87
	0.533	12.88
	1.331	9.89
705.01 (1.16)	2.961	3.38
	2.233	5.39
	1.616	7.38
	1.112	9.41
	0.620	11.41
	0.387	13.38
	0.215	15.36
	0.240	14.39
	0.426	12.43
	0.894	10.39
	1.309	8.46
	1.865	6.39
705.02 (0.802)	1.382	3.41
	0.743	5.39
	0.444	7.39
	0.231	9.41
	0.135	11.41
	0.173	10.38
	0.311	8.41
	0.565	6.41
	0.955	4.41
	1.781	2.51
705.03 (0.560)	1.981	2.51
	0.856	4.41
	0.355	6.38
	0.157	8.41
	0.102	9.41
	0.223	7.38
	0.533	5.41
	1.315	3.41
705.04 (0.393)	1.300	0.94
	0.489	2.88
	0.205	4.86
	0.081	6.91
	0.109	5.91
	0.268	3.91
	0.716	1.91
707.01 (0.968)	1.823	1.91
	1.183	3.88
	0.771	5.86
	0.633	7.89
	0.446	9.91
	0.284	11.89
	0.172	13.89
	0.196	12.86
	0.374	10.91
	0.521	8.88
	0.713	6.86
	0.936	4.91
	1.432	2.91
707.02 (0.671)	1.664	1.38
	0.803	3.38
	0.436	5.38
	0.223	7.41
	0.117	9.39
	0.173	8.38
	0.390	6.39
	0.831	4.39
	1.110	2.41
707.03 (0.470)	1.191	0.96
	0.664	2.36
	0.335	3.89
	0.166	5.36
	0.142	6.16
	0.249	4.66
	0.491	3.16
	0.831	1.66
707.04 (0.324)	0.545	0.91
	0.332	1.88
	0.185	2.89
	0.117	3.88
	0.095	4.41
	0.155	3.38
	0.235	2.39
	0.365	1.39
	0.572	0.44
713.01 (1.18)	2.715	2.93
	2.020	4.91
	1.634	6.89
	1.106	8.89
	0.869	10.89
	0.679	12.88
	0.330	14.89
	0.147	16.86
	0.254	15.89
	0.442	13.91
	1.165	9.91
	2.046	5.91
	2.583	3.88
713.02 (0.804)	1.079	3.88
	0.591	5.89
	0.346	7.91
	0.208	9.91
	0.137	10.91
	0.258	8.91
	0.470	6.88
	0.807	4.91
	1.315	2.93
	1.882	1.91
713.03 (0.558)	1.455	1.91
	0.612	3.91
	0.252	5.89
	0.097	7.91
	0.153	6.89
	0.406	4.91
	0.959	2.91
	2.239	0.88
717.01 (0.392)	1.622	0.88
	0.740	1.91
	0.388	2.93
	0.209	3.91
	0.140	4.86
	0.087	5.84
	0.132	5.36
	0.174	4.41
	0.306	3.39
	0.331	2.36
	0.474	1.41
	0.838	0.41
717.02 (0.328)	0.629	0.41
	0.347	1.39
	0.219	2.39
	0.131	3.41
	0.148	2.91
	0.234	1.91
	0.391	0.86
717.03 (0.468)	2.244	0.86
	0.652	2.38
	0.655	3.89
	0.337	5.38
	0.143	6.89
	0.132	7.64
	0.231	6.16
	0.441	4.66
	0.818	3.16
	1.575	1.66
717.04 (0.667)	1.978	3.38
	0.702	5.41
	0.303	7.39
	0.162	9.38
	0.157	8.39
	0.468	6.36
	1.170	4.41
721.01 (1.06)	2.717	1.91
	1.654	4.86
	0.980	7.89
	0.537	10.89
	0.238	13.91
	0.326	12.38
	0.736	9.39
	1.359	6.36
	2.370	3.38
721.02 (0.723)	1.890	1.41
	0.982	3.39
	0.522	5.36
	0.314	7.36
	0.149	9.39
	0.121	10.41
	0.198	8.41
	0.413	6.36
	0.750	4.36
	1.327	2.38
721.03 (0.502)	1.577	1.34
	0.634	3.38
	0.251	5.36
	0.106	7.39
	0.185	6.36
	0.375	4.36
	0.856	2.36
721.04 (0.352)	1.445	1.38
	0.920	2.36
	0.504	3.38
	0.284	4.37
	0.185	5.36
	0.202	4.86
	0.369	3.91
	0.668	2.91
	1.078	1.89
	1.791	0.88

Table A-2. Basic data, concentration distribution measurements, V_B = 0.035 foot per second, amplitude < 0.693 foot.

Curve No. (U_0, ft/s)	Concentration (g/l)	Elevation (cm)
621.01 (1.170)	1.417	3.39
	0.531	7.38
	0.095	11.41
	0.171	9.91
	1.076	5.88
	1.441	4.86
	0.323	8.87
621.02 (0.777)	2.127	2.43
	0.936	4.41
	0.360	6.38
	0.114	8.41
	0.041	9.36
	0.211	7.41
	0.492	5.43
	1.185	3.43
621.03 (0.537)	0.487	3.43
	0.256	5.38
	0.105	6.41
	0.284	4.38
	0.699	2.41
	1.037	1.41
	1.263	0.91
621.04 (0.375)	1.425	0.91
	0.529	2.88
	0.173	4.90
	0.148	5.59
	0.270	4.23
	0.371	3.63
	0.705	2.26
	0.977	1.61
621.05 (0.263)	0.383	1.61
	0.307	2.63
	0.237	3.63
	0.126	4.63
	0.136	4.11
	0.179	3.13
	0.283	2.11
	0.482	0.91
628.01 (0.263)	1.673	0.91
	1.095	1.91
	0.696	2.89
	0.348	3.91
	0.193	4.88
	0.116	5.88
	0.142	5.41
	0.260	4.41
	0.427	3.41
	0.723	2.41
	1.214	1.41
628.02 (0.376)	2.024	2.41
	0.631	4.41
	0.213	6.38
	0.075	8.41
	0.099	7.74
	0.154	7.11
	0.350	5.41
	0.855	3.76
	1.239	3.09
628.03 (0.558)	1.881	3.09
	0.697	4.91
	0.237	6.91
	0.074	8.91
	0.084	7.91
	0.340	5.91
	1.275	3.86
	1.613	3.41
	0.121	8.39
629.01 (0.780)	2.594	3.43
	1.028	5.38
	0.378	7.36
	0.175	9.38
	0.084	11.34
	0.119	10.38
	0.239	8.41
	0.593	6.41
	1.527	4.43
629.02 (1.177)	2.089	4.43
	1.166	6.83
	0.525	8.38
	0.269	10.39
	0.104	12.38
	0.143	11.36
	0.340	9.41
	0.674	7.41
	1.437	5.38
629.03 (0.947)	2.037	5.38
	1.121	7.39
	0.610	9.41
	0.288	11.41
	0.176	13.41
	0.225	12.43
	0.524	10.39
	0.728	8.41
	1.601	6.41
629.04 (0.448)	1.868	1.91
	0.654	3.91
	0.238	5.88
	0.072	7.91
	0.092	7.41
	0.171	6.38
	0.352	4.91
	0.722	3.41
	1.175	2.41
	1.814	1.41
711.01 (1.113)	2.484	0.94
	1.152	2.91
	0.506	4.88
	0.285	6.89
	0.197	8.91
	0.255	7.91
	0.402	5.91
	0.771	3.89
	2.148	1.91
711.02 (0.715)	2.112	0.91
	0.811	2.91
	0.376	4.91
	0.165	6.91
	0.089	7.91
	0.251	5.91
	0.584	3.89
	1.290	1.91
711.03 (0.487)	1.297	0.91
	0.607	2.41
	0.247	3.91
	0.122	5.39
	0.064	6.16
	0.157	4.66
	0.336	3.16
	0.792	1.66
	1.547	0.39
711.04 (0.337)	2.532	0.39
	1.542	1.41
	0.812	2.38
	0.490	3.38
	0.194	4.38
	0.228	3.91
	0.476	2.88
	1.024	1.91
	1.773	0.91
711.05 (0.405)	2.755	1.41
	1.810	2.39
	0.930	3.38
	0.311	4.43
	0.156	5.38
	0.222	4.91
	0.520	3.89
	1.226	2.93
	2.357	1.91
711.06 (0.583)	2.069	1.91
	0.822	3.41
	0.315	4.91
	0.097	6.36
	0.190	5.66
	0.512	4.18
	1.202	2.66
711.07 (0.890)	2.157	2.66
	0.559	4.41
	0.054	6.39
	0.101	5.91
	0.331	4.91
	0.876	3.91
	1.869	2.93
802.01 (0.570)	2.471	0.44
	1.246	1.19
	0.356	1.98
	0.094	2.81
	0.062	3.21
	0.191	2.36
	0.621	1.61
	2.025	0.80
802.02 (0.452)	0.802	0.80
	0.468	1.59
	0.214	2.36
	0.067	3.21
	0.134	2.78
	0.348	1.96
	0.585	1.21
	1.232	0.36
802.03 (0.363)	1.717	0.36
	0.593	1.21
	0.225	1.98
	0.116	2.81
	0.093	3.21
	0.162	2.41
	0.305	1.56
	0.856	0.82
802.04 (0.247)	0.930	0.36
	0.412	1.01
	0.166	1.59
	0.068	2.21
	0.101	1.86
	0.218	1.31
	0.538	0.75
802.05 (0.297)	1.994	0.33
	0.572	1.21
	0.172	1.96
	0.069	2.81
	0.098	2.39
	0.326	1.56
	1.150	0.81
814.01 (0.585)	2.533	0.36
	1.695	1.38
	0.826	2.41
	0.504	3.39
	0.288	4.38
	0.163	5.36
	0.085	6.36
	0.115	5.86
	1.803	0.88
814.02 (0.585)	2.168	0.36
	1.297	1.92
	0.756	3.34
	0.349	4.89
	0.126	6.34
	0.255	5.66
	0.562	4.11
	1.019	2.62
	1.592	1.16
814.03 (0.585)	1.829	0.36
	1.227	1.91
	0.721	3.41
	0.302	4.88
	0.162	6.34
	0.198	5.64
	0.558	4.12
	0.859	2.63
	1.464	1.11
814.04 (0.585)	1.804	0.39
	0.857	1.86
	0.436	3.36
	0.234	4.89
	0.074	6.34
	0.110	5.66
	0.293	4.14
	0.562	2.64
	1.183	1.13
814.05 (0.585)	1.898	0.34
	1.303	1.89
	0.776	3.37
	0.384	4.88
	0.116	6.38
	0.169	5.66
	0.499	4.14
	0.907	2.64
	1.472	1.16

Table A-3. Basic data, concentration distribution measurements, V_s = 0.0498 foot per second, amplitude = 0.848 foot.

Curve No. (U_o, ft/s)	Concentration (g/l)	Elevation (cm)	Curve No. (U_o, ft/s)	Concentration (g/l)	Elevation (cm)	Curve No. (U_o, ft/s)	Concentration (g/l)	Elevation (cm)	Curve No. (U_o, ft/s)	Concentration (g/l)	Elevation (cm)
927.01	1.725	2.70	927.02	1.932	1.53	927.03	1.527	1.03	927.04	0.620	1.53
(1.08)	1.100	4.50	(0.850)	1.004	3.51	(0.682)	0.921	2.03	(0.558)	0.425	2.53
	0.680	6.48		0.479	5.50		0.638	3.03		0.256	3.48
	0.454	8.43		0.261	7.48		0.408	4.02		0.335	2.93
	0.271	10.50		0.211	8.51		0.294	5.03		0.479	2.03
	0.360	9.51		0.322	6.50		0.383	4.50		0.724	1.01
	0.523	7.53		0.650	4.50		0.494	3.50			
	0.882	5.48		1.194	2.48		0.759	2.53			
	1.353	3.53					1.042	1.53			
	2.062	1.53									

Table A-4. Basic data, concentration distribution measurements, V_s = 0.626 foot per second, amplitude = 1.25 feet.

Curve No. (U_o, ft/s)	Concentration (g/l)	Elevation (cm)	Curve No. (U_o, ft/s)	Concentration (g/l)	Elevation (cm)	Curve No. (U_o, ft/s)	Concentration (g/l)	Elevation (cm)	Curve No. (U_o, ft/s)	Concentration (g/l)	Elevation (cm)
913.01	3.064	0.67	913.02	2.190	0.70	913.03	1.194	0.85	913.04	0.473	1.12
(1.082)	1.140	3.62	(0.758)	0.517	3.65	(0.530)	0.708	1.62	(0.437)	0.287	2.15
	0.602	6.62		0.226	6.60		0.454	2.62		0.213	2.62
	0.376	9.65		0.257	5.60		0.269	3.62		0.355	1.65
	0.385	11.12		0.372	4.64		0.314	3.17		0.643	0.67
	0.498	8.16		0.855	2.65		0.515	2.12			
	0.812	5.14		1.248	1.60		0.863	1.12			
	1.685	2.17									

Table A-5. Basic data, turbulence velocity distribution measurements, amplitude = 0.925 foot.

Curve No. (U_o, ft/s)	Velocity scale (ft/s)	Elevation (ft)	Curve No. (U_o, ft/s)	Velocity scale (ft/s)	Elevation (ft)	Curve No. (U_o, ft/s)	Velocity scale (ft/s)	Elevation (ft)	Curve No. (U_o, ft/s)	Velocity scale (ft/s)	Elevation (ft)
112.01	0.0675	0.0342	112.02	0.0826	0.0258	112.03	0.0645	0.0550	112.04	0.1048	0.0258
(0.353)	0.0358	0.0850	(0.510)	0.0512	0.0835	(0.748)	0.0477	0.0840	(0.930)	0.0955	0.0258
	0.0273	0.1260		0.0320	0.124		0.0265	0.126		0.0492	0.0835
	0.0129	0.1675		0.0207	0.167		0.0194	0.168		0.0360	0.126
	0.00975	0.2090		0.0108	0.208		0.0130	0.209		0.0205	0.167
	0.0157	0.1880		0.00763	0.250		0.00735	0.251		0.0133	0.210
	0.0156	0.1470		0.0105	0.230		0.0132	0.273		0.0120	0.251
	0.0340	0.1040		0.0135	0.188		0.00953	0.230		0.0130	0.273
	0.0392	0.0592		0.0278	0.146		0.00981	0.188		0.0145	0.230
	0.0652	0.0259		0.0373	0.104		0.0212	0.148		0.0163	0.188
				0.0619	0.0550		0.0367	0.104		0.0273	0.146
							0.0860	0.0258		0.0407	0.104
										0.0692	0.0592

MacDonald, Thomas C.
Sediment suspension and turbulence in an oscillating flume / by Thomas C. MacDonald. – Fort Belvoir, Va. : U.S. Coastal Engineering Research Center, 1977.
80 p. : ill. (Technical paper - Coastal Engineering Research Center; no. 77-4) Also (Contract - Coastal Engineering Research Center ; DACW72-71-C-0024)
Bibliography: p. 74.
In 65 experiments with one lightweight sediment, suspended-sediment concentration was linear with elevation, except near the bottom, as found by others. In limited experiments with different fall velocities, slope of the concentration distribution becomes more negative as fall velocity increases. RMS velocity fluctuations were also measured.
1. Sediment suspension. 2. Turbulence. 3. Waves. 4. Flumes. I. Title. II. Series: U.S. Coastal Engineering Research Center. Technical paper no. 77-4. III. Series: U.S. Coastal Engineering Research Center. Contract DACW72-71-C-0024.

TC203 .U581tp no. 77-4 627

MacDonald, Thomas C.
Sediment suspension and turbulence in an oscillating flume / by Thomas C. MacDonald. – Fort Belvoir, Va. : U.S. Coastal Engineering Research Center, 1977.
80 p. : ill. (Technical paper - Coastal Engineering Research Center; no. 77-4) Also (Contract - Coastal Engineering Research Center ; DACW72-71-C-0024)
Bibliography: p. 74.
In 65 experiments with one lightweight sediment, suspended-sediment concentration was linear with elevation, except near the bottom, as found by others. In limited experiments with different fall velocities, slope of the concentration distribution becomes more negative as fall velocity increases. RMS velocity fluctuations were also measured.
1. Sediment suspension. 2. Turbulence. 3. Waves. 4. Flumes. I. Title. II. Series: U.S. Coastal Engineering Research Center. Technical paper no. 77-4. III. Series: U.S. Coastal Engineering Research Center. Contract DACW72-71-C-0024.

TC203 .U581tp no. 77-4 627

MacDonald, Thomas C.
Sediment suspension and turbulence in an oscillating flume / by Thomas C. MacDonald. – Fort Belvoir, Va. : U.S. Coastal Engineering Research Center, 1977.
80 p. : ill. (Technical paper - Coastal Engineering Research Center; no. 77-4) Also (Contract - Coastal Engineering Research Center ; DACW72-71-C-0024)
Bibliography: p. 74.
In 65 experiments with one lightweight sediment, suspended-sediment concentration was linear with elevation, except near the bottom, as found by others. In limited experiments with different fall velocities, slope of the concentration distribution becomes more negative as fall velocity increases. RMS velocity fluctuations were also measured.
1. Sediment suspension. 2. Turbulence. 3. Waves. 4. Flumes. I. Title. II. Series: U.S. Coastal Engineering Research Center. Technical paper no. 77-4. III. Series: U.S. Coastal Engineering Research Center. Contract DACW72-71-C-0024.

TC203 .U581tp no. 77-4 627

MacDonald, Thomas C.
Sediment suspension and turbulence in an oscillating flume / by Thomas C. MacDonald. – Fort Belvoir, Va. : U.S. Coastal Engineering Research Center, 1977.
80 p. : ill. (Technical paper - Coastal Engineering Research Center; no. 77-4) Also (Contract - Coastal Engineering Research Center ; DACW72-71-C-0024)
Bibliography: p. 74.
In 65 experiments with one lightweight sediment, suspended-sediment concentration was linear with elevation, except near the bottom, as found by others. In limited experiments with different fall velocities, slope of the concentration distribution becomes more negative as fall velocity increases. RMS velocity fluctuations were also measured.
1. Sediment suspension. 2. Turbulence. 3. Waves. 4. Flumes. I. Title. II. Series: U.S. Coastal Engineering Research Center. Technical paper no. 77-4. III. Series: U.S. Coastal Engineering Research Center. Contract DACW72-71-C-0024.

TC203 .U581tp no. 77-4 627

MacDonald, Thomas C.
Sediment suspension and turbulence in an oscillating flume / by Thomas C. MacDonald. – Fort Belvoir, Va. : U.S. Coastal Engineering Research Center, 1977.
80 p. : ill. (Technical paper - Coastal Engineering Research Center; no. 77-4) Also (Contract - Coastal Engineering Research Center ; DACW72-71-C-0024)
Bibliography: p. 74.
In 65 experiments with one lightweight sediment, suspended-sediment concentration was linear with elevation, except near the bottom, as found by others. In limited experiments with different fall velocities, slope of the concentration distribution becomes more negative as fall velocity increases. RMS velocity fluctuations were also measured.
1. Sediment suspension. 2. Turbulence. 3. Waves. 4. Flumes. I. Title. II. Series: U.S. Coastal Engineering Research Center. Technical paper no. 77-4. III. Series: U.S. Coastal Engineering Research Center. Contract DACW72-71-C-0024.

TC203 .U581tp no. 77-4 627

MacDonald, Thomas C.
Sediment suspension and turbulence in an oscillating flume / by Thomas C. MacDonald. – Fort Belvoir, Va. : U.S. Coastal Engineering Research Center, 1977.
80 p. : ill. (Technical paper - Coastal Engineering Research Center; no. 77-4) Also (Contract - Coastal Engineering Research Center ; DACW72-71-C-0024)
Bibliography: p. 74.
In 65 experiments with one lightweight sediment, suspended-sediment concentration was linear with elevation, except near the bottom, as found by others. In limited experiments with different fall velocities, slope of the concentration distribution becomes more negative as fall velocity increases. RMS velocity fluctuations were also measured.
1. Sediment suspension. 2. Turbulence. 3. Waves. 4. Flumes. I. Title. II. Series: U.S. Coastal Engineering Research Center. Technical paper no. 77-4. III. Series: U.S. Coastal Engineering Research Center. Contract DACW72-71-C-0024.

TC203 .U581tp no. 77-4 627

MacDonald, Thomas C.
Sediment suspension and turbulence in an oscillating flume / by Thomas C. MacDonald. – Fort Belvoir, Va. : U.S. Coastal Engineering Research Center, 1977.
80 p. : ill. (Technical paper - Coastal Engineering Research Center; no. 77-4) Also (Contract - Coastal Engineering Research Center ; DACW72-71-C-0024)
Bibliography: p. 74.
In 65 experiments with one lightweight sediment, suspended-sediment concentration was linear with elevation, except near the bottom, as found by others. In limited experiments with different fall velocities, slope of the concentration distribution becomes more negative as fall velocity increases. RMS velocity fluctuations were also measured.
1. Sediment suspension. 2. Turbulence. 3. Waves. 4. Flumes. I. Title. II. Series: U.S. Coastal Engineering Research Center. Technical paper no. 77-4. III. Series: U.S. Coastal Engineering Research Center. Contract DACW72-71-C-0024.

TC203 .U581tp no. 77-4 627

MacDonald, Thomas C.
Sediment suspension and turbulence in an oscillating flume / by Thomas C. MacDonald. – Fort Belvoir, Va. : U.S. Coastal Engineering Research Center, 1977.
80 p. : ill. (Technical paper - Coastal Engineering Research Center; no. 77-4) Also (Contract - Coastal Engineering Research Center ; DACW72-71-C-0024)
Bibliography: p. 74.
In 65 experiments with one lightweight sediment, suspended-sediment concentration was linear with elevation, except near the bottom, as found by others. In limited experiments with different fall velocities, slope of the concentration distribution becomes more negative as fall velocity increases. RMS velocity fluctuations were also measured.
1. Sediment suspension. 2. Turbulence. 3. Waves. 4. Flumes. I. Title. II. Series: U.S. Coastal Engineering Research Center. Technical paper no. 77-4. III. Series: U.S. Coastal Engineering Research Center. Contract DACW72-71-C-0024.

TC203 .U581tp no. 77-4 627